Statistics of the Geomagnetic Secular Variation for the past 5Ma

C.G. Constable & R.L. Parker,

Institute of Geophysics & Planetary Physics,

Scripps Institution of Oceanography,

University of California, San Diego,

La Jolla CA 92093.

Abstract

A new statistical model is proposed for the geomagnetic secular variation over the past 5Ma. Unlike previous models, which have been based on the assumption of a Fisher distribution for either VGP positions and/or field directions, the model makes use of statistical characteristics of the present day geomagnetic field. The spatial power spectrum of the non-dipole field is consistent with a white source near the core-mantle boundary with Gaussian distribution. After a suitable scaling, the spherical harmonic coefficients may be regarded as statistical samples from a single giant Gaussian process; this is our model of the non-dipole field. We can combine this model with an arbitrary statistical description of the dipole and compute the probability density functions and cumulative distribution functions for declination and inclination that would be observed at any site on the surface of the Earth. Global paleomagnetic data spanning the past 5Ma are used to constrain the statistics of the dipole part of the field. A simple model is found to be consistent with the available data: (a) with two exceptions, each Gauss coefficient is independently normally distributed with zero mean and standard deviation for the non-dipole terms commensurate with a white source at the core surface; (b) the exceptions are the axial dipole, g_1^0, and axial quadrupole, g_2^0, terms; the axial dipole distribution is bimodal and symmetric, resembling a combination of two normal distributions with centers close to the present-day value, and its sign-reversed counterpart; (c) the standard deviations of the non-axial dipole terms, g_1^1 and h_1^1,

and of the magnitude of the axial dipole are all about 10% of the present-day g_1^0 component; (d) the axial quadrupole reverses sign with the axial dipole and has a mean magnitude of 6% of its mean. An advantage of specifying the model in terms of the spherical harmonic coefficients is that it is a complete statistical description of the geomagnetic field, enabling us to test specific properties for a general description; both intensity and directional data distributions may be tested to see if they satisfy the expected model distributions.

Introduction

It is by now generally accepted that the geomagnetic field is generated by some sort of dynamo process in the Earth's core (see *e.g.*, Moffatt, 1978). The field is by no means constant; changes on time scales from ten years to ten thousand years are classified as secular variations. Such fluctuations are consequences of the nonsteady nature of the field-producing mechanism within the core. More rapid variations, if they exist, cannot be detected because of screening due to mantle conductivity and interference from fluctuations of external origin. At the longer periods, it is difficult to dissociate mere secular variation from the actual reversal of the main field and it is quite possible the distinction is artificial. Unfortunately, the theory of the geo-dynamo is not currently in an advanced enough state to make more than the simplest predictions about the paleofield variation (*e.g.*, Merrill and McElhinny, 1983, Chapter 9). When a system is as complex in space and time as the geomagnetic field, it is a natural and efficient strategy to call upon some kind of statistical characterization of it to uncover general properties, rather than to attempt a description of the behavior of the system at every instant and at all points. Previous statistical descriptions of the paleomagnetic field have centered around the use of Fisher statistics (Fisher, 1953) and attempts to describe the observed variation in geomagnetic field dispersion (from paleomagnetic data) as a function of latitude (Creer *et al.* 1959; Creer 1962; Cox 1962, 1970; Baag & Helsley 1974; McElhinny & Merrill 1975; Harrison 1980; McFadden & McElhinny 1984). The most successful of these to date has been the so-called Model F of McFadden & McElhinny (1984), for which the average intensity of non-dipole components of the field at any latitude are assumed proportional to that of the dipole field, and the angular distribution of VGP

directions is assumed to exhibit axial symmetry. The model provides a good fit to the variation in VGP angular dispersion as a function of latitude. The aim of this work is to provide a statistical description of the field variation, by combining the properties of the present-day field and of paleomagnetic measurements. This statistical description does not just describe the angular dispersion expected at any latitude, but provides complete statistical distributions expected for the secular variation at any site on the Earth's surface. The resulting models are specified in terms of the spherical harmonic coefficients describing the geomagnetic field.

The general plan of this paper is as follows. Two kinds of data describing the main geomagnetic field each supply components of the model and these are discussed; they are the modern data, with their excellent geographical coverage of the Earth, and the paleosecular variation data which span long time periods, but in general have poor global coverage. The modern data provide a good estimate of the spatial power spectrum of the geomagnetic field, and enable us to show that the non-dipole part of the field is consistent with a white source near the core-mantle boundary. By suitable scaling of the spherical harmonic coefficients it is possible to regard them as statistical samples from a single giant Gaussian distribution. Supposing that a kind of uniformitarianism has held true, we assume that this giant Gaussian process has always been a good description for the non-dipole geomagnetic field. However, the modern data cannot help us with the statistical variation of the dipole, which involves much longer time spans; we must use paleodata to study its behavior. Using a statistical framework it is possible to predict the cumulative distribution functions for quantities related to inclination and declination, which are the most accurately measured paleodata. The paleodata provide us with empirical cumulative distribution functions for the directional data from Hawaii and Iceland, where there are extensive paleosecular variation data from lava flows, and also for a global data set based on a compilation by Lee (1983). We construct a simple model with a number of free parameters, and adjust them to reconcile the model and the paleodata.

1. Short-Term Data and Nondipole Field Statistics

Satellite and observatory measurements and historical records of the geomagnetic field fall into the category of short-term secular variation data. Observatory data rarely extend back more than 100 years, but provide reasonable simultaneous global coverage for that time (although the distribution of sites is heavily biased towards the northern hemisphere and Europe, and permanent observatories are necessarily restricted to land which is very unevenly distributed over the surface of the Earth). Satellite measurements have been performed at irregular intervals since the launch of Sputnik 3 in 1958 (see Langel, 1985 for a complete list), and the resulting data have varied in quality and extent of global coverage. Magsat (Langel *et al.*, 1980, 1982) provided the first truly global survey of the vector components of the geomagnetic field.

The method of analysis for these data was devised in 1838 by Gauss and involves representing the geomagnetic field of internal origin as the gradient of a potential Ψ whose spatial variation is specified by an infinite sum of spherical harmonics.

$$\Psi = a \sum_{l=1}^{\infty} \sum_{m=0}^{l} (\frac{a}{r})^{l+1}(g_l^m \cos m\phi + h_l^m \sin m\phi)P_l^m(\cos\theta)$$

g_l^m and h_l^m are known as the Schmidt partially normalized Gauss coefficients and provide a complete description of the geomagnetic field. Appendix 1 gives the relationships between fully and partially normalized spherical harmonic representations and indicates how they are computed. In this work we make use of the GSFC980 spherical harmonic model of Langel *et al.* (1980), derived from Magsat data.

Previous secular variation studies have been seriously hampered by an inability to handle the non-dipole components of the field in a quantitative manner. We propose a way out of the difficulty based upon a simple observation of the present-day field, that the non-dipole terms can be described by a zero-mean Gaussian process, and that it is plausible to assume this property has held for all time.

Mauersberger (1956) first defined a kind of geomagnetic power spectrum based on the spherical harmonic expansion of the geomagnetic field. Subsequently, other workers have used various

forms for the spectrum with different weighting as a function of degree. Here the form devised by Lowes (1974) is used. For each spherical harmonic of degree l, the power at radius r is R_l,

$$R_l\ (r) = (\frac{a}{r})^{2(l+2)}(l+1) \sum_{m=0}^{l} \{ (g_l^m)^2 + (h_l^m)^2 \}$$

where g_l^m and h_l^m are the Gauss coefficients in the Schmidt quasi-normalized spherical harmonic expansion. Equivalently,

$$R_l = <B_l \cdot B_l>$$

where B_l is the magnetic field associated with degree l in the expansion and $< >$ denotes the average over the surface of the Earth.

At the Earth's surface the spectrum drops exponentially with a slope indicating a white source approximately at the core's surface (see Figure 1). Lowes gives:

$$R_l \approx 4.0 \times 10^3 \ (4.5)^{-l} (\mu T)^2$$

The deviations from this law for $l > 8$ are thought to represent power from crustal magnetization. The spectrum has subsequently been refined, through the use of the more complete Magsat data set (Langel & Estes 1982). They estimate that the spectrum is consistent with a white source 174 km below the seismic core-mantle boundary.

If the spectrum of the geomagnetic field were precisely the same throughout geologic time then secular variation would just be reflected by a rearrangement within the individual g_l^m and h_l^m while the power R_l remained constant. This implies a kind of $2l+1$-dimensional Fisherian distribution for the Gauss coefficients. However, exactly constant power in each spherical harmonic degree contradicts observation; continual small changes in R_l are undoubtedly occurring. We therefore choose a description in which the power is also a random variable. The simplest model treats the individual spherical harmonic coefficients as normally distributed random variables. This simple model or a similar assumption has been used by other workers as a statistical description of the secular variation (see *e.g.*, Gubbins, 1983, Eckhardt, 1984) and has some very attractive features. For example, the statistical prescription is invariant under reorientation of the coordinate axes. Many other specifications force a privileged status on one particular axis system,

something that is clearly undesirable. Another attractive feature is that the model is amenable to testing, at least for the present day field.

We use the Lowes spectrum as a *guide* in construction of our statistical model. For the non-dipole terms we choose a model spectrum that is exactly flat at the surface of the core:

$$E\{R_l\} = E\{ \sum_{m=0}^{l} (l+1) [(g_l^m)^2 + (h_l^m)^2]\}$$

$$= (c/a)^{2l}\alpha^2, \qquad l \geq 2$$

where E{ } is the expectation of the parameter in the brackets, c/a is the ratio of the core radius to that of the Earth (0.547) and $\alpha=27.7\mu T$ is a fitted parameter. In addition we assume that within each degree l, g_l^m and h_l^m are independent identically distributed normal random variables of zero mean. If $var(h_l^m) = var(g_l^m) = \sigma_l^2$ then

$$\sigma_l^2 = \frac{(c/a)^{2l}\alpha^2}{(l+1)(2l+1)}$$

If we define scaled Gauss coefficients

$$\bar{g}_l^m = v_l g_l^m$$

$$\bar{h}_l^m = v_l h_l^m$$

where $v_l^2=(l+1)(2l+1)(a/c)^{2l}$, then these coefficients (which completely characterize the non-dipole field for statistical purposes) are just independent samples of a single zero-mean Gaussian process with variance α^2. Even though there is some evidence to indicate that the level at which the spectrum is white lies somewhat below the core mantle boundary we prefer to characterize the spectrum in terms of the known physical constants c and a. The reason for this is that we do not believe that the true level is very well constrained. In any case, the method used here in fitting the data yields an excellent fit to both the spectrum (see the straight line fit on Figure 1) and, as we will see, the Gaussian distributional form for the non-dipole field. Subsequently, we may want to allow the level where the spectrum appears white to vary. This may be done by changing the variance α^2 of the scaled Gaussian distribution.

The spherical harmonic field coefficients for 1980 (GSFC980) data for degree $l = 2$ through to $l = 8$ or higher may be used to test whether this Gaussian distribution is actually observed in the appropriately scaled coefficients. Figure 2 shows the cumulative distribution versus the theoretical normal curve. The agreement between the two curves is impressive. While there is no means of determining a unique statistical model from so few data, it is possible to test whether a data sample is consistent with an assumed distribution. The Kolmogorov-Smirnov test (see $e.g.$ Massey 1951, Kendall & Stuart, 1979) is a powerful means of determining probabilistic bounds within which samples from a particular theoretical distribution function should lie; one virtue of it is that the test itself is independent of the underlying theoretical distribution function (although of course this must be known to compute the discrepancy statistic d_N). The data of Figure 2 are consistent with an underlying normal distribution for the non-dipole field; they exhibit a maximum discrepancy from the theoretical normal distribution of $d_N = .061$, where $N = 77$. However, if the three dipole terms associated with $l = 1$ are included, we find the K-S test for normality fails, demonstrating that the dipole terms do not follow the same pattern as the rest of the field. One might suspect that just the axial ($i.e.$, g_1^0) part of the dipole field is anomalous and we can test this by including the non-axial dipole terms (g_1^1 and h_1^1) in the tested distribution. Then the population tests out as Gaussian at the same level as the non-dipole field. Therefore it appears that according to this model, only the axial dipole term g_1^0 is anomalous.

As a description of the non-dipole field, our model has simplicity and economy; only one number, the variance, needs to be determined empirically. It seems extremely unlikely that such a simple description is an accident and pertains to today's field alone. Rather, it is a reasonable working hypothesis that this model accurately provides the statistics of the non-dipole part of the paleofield as well. Now, for example, we can compute the statistics of the "noise" contributed to paleomagnetic measurements due to non-dipole sources. From the spherical harmonic representation we can show 1) that the components of the non-dipole field at the Earth's surface are also independent Gaussian variables with zero means, 2) that the variances of the horizontal components locally are equal, and 3) that they are different from that of the vertical component.

This is done in Appendix 2. The inequality of the vertical and horizontal variances makes it evident that the distribution of directions for the non-dipole part of the field is not Fisherian. This is entirely consistent with observation.

2. Paleodata and the Dipole Field

With paleomagnetic data it is never possible to obtain the detailed instantaneous description of the magnetic field that we have for the present day. However, we can obtain information about much longer term variations, which is essential for a description of the dipole part of the field variation. The bulk of the data available consists of directional measurements of the paleomagnetic field. Measurements of the absolute paleointensity of the Earth's magnetic field can be obtained from lava flows and baked archeomagnetic materials. Such measurements are exceedingly time consuming and therefore are far less numerous than directional measurements. Nevertheless, they are important if we are to be able to determine average values of field intensity as well as direction. The available data have been compiled by McElhinny & Senanayake (1982) for the past 50 thousand years and by McFadden & McElhinny (1982) for the past 5Ma. For directional data, there are two major sources of paleodata that span long time periods, lava flows and sedimentary sequences.

Samples from lava flows typically produce very high quality data, but have the disadvantage that they only provide instantaneous recordings of the field properties at the time of acquisition of the remanence. This is not, however, an insurmountable problem for a statistical model of the geomagnetic field, since we are seeking a probability distribution rather than a deterministic model of magnetic field changes with time. Precise age control is not necessary, nor indeed is a continuous record of the field; all that is required is that we obtain a representative sample of the complete range of the secular variation at a given site. There are two places which could conceivably offer sufficient data, namely Hawaii and Iceland. Both islands have experienced repeated volcanic eruptions at relatively short time intervals over the past few million years. Extensive data sets are available from these sites already (for Hawaii see Doell and Cox, 1965; Doell, 1969; Doell, 1972a,b,c; Doell and Dalrymple, 1973; for Iceland see Watkins, McDougall and Kristjansson,

1977; Kristjansson *et al.*, 1980). From the pool of declination and inclination data for each of these sites, we can obtain empirical cumulative distribution functions (cdfs) for declination and inclination at the latitude for each of these sites. Figure 3 shows these empirical functions, for Hawaii using the data of Doell & Cox (1965), Doell (1972a,b,c) and Doell & Dalrymple (1973), and for Iceland using the data of Watkins, McDougall & Kristjansson (1977) and Kristjansson *et al.* (1980). Data from lavas more than 5Ma old were excluded as were those sites with Fisherian $\alpha_{95} > 20°$, in order to reduce contamination of the secular variation signal by tectonic movements and rock magnetic noise. The inclination data are all mapped onto the lower hemisphere in order to avoid the necessity of deciding whether they correspond to a normal or reversed field and the declinations are mapped into the range $-90° < d \leq 90°$. This could be important for low latitude sites, where secular variation might result in an apparent field reversal. The changes of variable from declination D and inclination I to their modified forms d and i are performed as follows.

$$i = |I|$$

and

$$d = D \quad \text{for } -90° < D \leq 90°$$
$$d = D + 180 \quad \text{for } -180° < D \leq -90°$$
$$d = D - 180 \quad \text{for } 90° < D \leq 180°$$

The other data we have employed comes from the global compilation by Lee (1983) for the past 5Ma, which contains about 1100 individual site measurements (as well as many more average results not used here), from a mixture of both sedimentary and igneous rocks. In the original selection of data for this compilation, data with $\alpha_{95} > 20°$ were excluded as were those with VGP latitudes of less than 45°. This is because low VGP latitudes were considered more likely to correspond to anomalous field behavior (Lee, 1983) and the object of the study was to look at "normal" secular variation. There are comparatively few sites where there are as many data as for Hawaii and Iceland, so generally we have to combine data from a number of different sites and obtain cdfs that are averages over a finite latitude band. This will also have the effect of averaging out non-zonal effects in the secular variation, which might otherwise be a problem even for very long records at a single site. Figure 4 shows the empirical cdfs for i, the absolute value of

the inclination, when the data are averaged in 8 latitude bands ranging in width from 2° to 9°. The northern and southern hemispheres are assumed to be symmetric in their behavior so that data from equivalent latitudes in the two hemispheres have been combined to yield a better estimate for the cdfs. This assumption of symmetry, means that any non-zero mean in the odd order terms in the spherical harmonic expansion will not be detected. The data distribution is such that very few of these bands contain sufficient data to provide an acceptable looking cdf. We would expect the cdf to look smooth, and many of these are jagged in shape, especially near the tails of the distribution. Two of the bands (11–13° and 52–54°) each only contain data from one or two locations and have only 51 and 62 field measurements respectively, and so can hardly be expected to sample the whole range of secular variation. In order to quantify the variation in the cdfs as a function of latitude we can look at the variation of the expectation and standard deviation of these distributions. These are computed by numerical integration of the empirical cdfs using a cubic spline quadrature scheme. In the upper part of Figure 5 are plotted the standard deviations, $\sigma(d)$ and $\sigma(i)$, respectively for d (triangles) and i (squares) for each of the latitude bands, whose cdfs are given in Figure 4. In the lower part is plotted the bias, B{i}, in the absolute value of the inclination. This is defined as the expected value of the absolute value of the inclination as computed from the empirical cdf minus the inclination that would be observed at that latitude if the field were due to an axial geocentric dipole. The axial dipole inclination is readily computed by

$$i_{ax} = \tan^{-1}(2\tan\lambda)$$

where λ is the latitude at the location in question. (Here the average latitude for the band, weighted by the number of data at each point, has been used.) Thus the bias is

$$B\{i\} = E\{i\} - i_{ax}$$

Some idea of the reliability of these distribution parameter estimates may be obtained by using a bootstrap technique (of the type reviewed by Efron & Tibshirani, 1986) to estimate one standard error in the parameters. The bootstrap method supposes that the distributions of Figure 4 represent the true underlying distribution of the secular variation data, and finds the standard error in the parameter estimate by repeated random resampling from this distribution, computing

the parameter estimate for each sample and then finding the sample standard deviation. The error bars for the parameters in Figure 5 are one standard error based on 500 bootstrap samples from each of the distributions shown in Figure 4. How good these bootstrap estimates of standard error are will of course depend on how well the distribution functions of Figure 4 represent the range of secular variation.

The general picture that emerges for the parameters of the cdfs of Figure 4 is that the inclination standard deviation rises from about 10° at the equator to around 13° at around a latitude of 25° and then slowly decreases with increasing latitude. It should be noted that mapping inclination onto the lower hemisphere results in a modified inclination standard deviation at the equator that is expected to be one half that of the true inclination. The declination standard deviation increases fairly steadily with latitude as does its uncertainty computed by the bootstrap. The solid lines connecting the data on this figure are cubic spline interpolation between data points and serve merely to guide the eye. The bias in the inclination is high near the equator (this is a consequence of mapping all the inclinations onto the lower hemisphere), but becomes consistently negative for latitudes higher than 7 or 8°. The size of the bootstrap error bars suggests that is would be optimistic to try and interpret the detailed variations in bias with increasing latitude.

Both the cdfs with the smallest number of points had somewhat smaller standard deviations in comparison with their nearest neighbors in latitude (marked by different symbols in Figure 5), and this aroused some suspicion that perhaps the samples were not large enough to contain the whole range of secular variation. To check this the data were combined into larger latitude bands. In Figure 6 cdfs for the absolute values of inclinations in latitude bands of 15° (for latitudes 0—45° and a band 25° wide for the highest latitudes) are plotted. These are much smoother than the cdfs obtained in Figure 4, and we can feel more secure that they represent an adequate sample for the variation. The price paid is that of resolution, the modified inclination standard deviations, $\sigma(i)$, computed for these distributions will be increased relative to those obtained before, because the expected value for the inclination distribution increases with latitude. The

standard deviations and bias for this grouping of the data are shown in Figure 7. They are similar in form to those obtained in Figure 5, but without some of the high frequency variation seen there. This supports the idea that some of the features in Figure 5 are an artifact of the small number of points used to compute the cdf in some latitude bands.

The next question that arises is whether this global data set is consistent with those from Hawaii and Iceland. Comparison of the Hawaiian data with that from the corresponding latitude band shows them to be quite similar. The global inclination data has a bias of -3.2° compared with -4.5° for Hawaii, and the standard deviations are quite similar, 12.0° and 13.2° respectively. The same is not true for the Iceland cdf which has a bias of -8.8° and a standard deviation of 11.8°, compared with a bias of -5.4° and standard deviation of 7.4° for the global data. A look at the source of the Icelandic data reveals that there are far more low inclination values than would have been expected from the global data set. The cdf for the Icelandic data has risen to a value of 0.2 already for inclinations of 60°, while for the global data set this does not occur until past 65°. This may be a consequence of the fact that in the global data set sites at which the VGP latitude lies below 45° are excluded, while we have made no such requirement in our compilation. However, inspection of the original data reveals that for the Icelandic data about 10% of the data corresponds to VGP latitudes that are less than 45°. If we assume that the lava flows are uniformly distributed in time, and that VGP latitudes this low correspond to times when the field was in transition between polarities, then this implies that the field spends 10% of its time in transition, or 0.32Ma out of the 3.2 Ma spanned by these two records. There are 15 reversals recorded in these lavas, thus if the extrusion rate was uniform, then on average the directional part of the magnetic field took about 20 thousand years to complete a reversal. This is significantly longer than the average time reversals are believed to take, *i.e.*, between 1 and 10thousand years (Merrill & McElhinny 1983, p164), although Clement & Kent, 1984, suggest that there is some evidence that reversals appear to take longer (by a factor of about two) at higher latitudes than near the equator. However, the Icelandic cdf could be heavily biased by non-uniform sampling of the field in time due to the erratic nature of the eruptions.

A complete description of the statistics of the magnetic field must include time scales long enough for reversals, but we hope they will not be so long that the underlying processes must be regarded as non-stationary. We choose the past 5Ma as a representative sample for the secular variation. This spans about 20 polarity changes (see *e.g.*, Merrill & McElhinny 1983, p.140), but is not so long that we have to take into account the effects of continental drift. The primary paleodata set that we hope to satisfy with our statistical model of the field consists of those data from the global data set compiled by Lee (1983) for which individual site measurements are available.

2.1. A Statistical Distribution for the Dipole Field

From now on we shall assume that a giant Gaussian process of the type described in Section 1 is an adequate description for the statistical variations in the non-dipole part of the field. The question now arises as to what is an appropriate model for the dipole field. This is, in fact, the major question addressed in this work. It is not a trivial matter, and indeed, a large part of the science of paleomagnetism is devoted to exactly this question: how does the dipole of the geomagnetic field behave? As we have been doing all along, we will ignore questions of development with time and concentrate instead on the statistical distribution of the dipole field amongst its various possible states.

Several approaches may be taken to modeling the dipole field variations. These will be discussed in order of increasing complexity. In all of the following models (with one exception) it will be assumed that the dipole part of the field is statistically independent of the non-dipole part. This is clearly not true in general; the complex evolution of secular variation must be controlled by the geodynamo, in which the dipole and non-dipole variations are presumably inextricably linked. However, in developing a statistical model for the secular variation we will make use of paleomagnetic data, which provides a sporadic sampling of the process throughout time. The assumption of independence is then like proposing there exists no requirement for the quadrupole term to always be small when the dipole term is large, or similar relationships between other spherical harmonic coefficients. Assuming that the data are not serially correlated

(certainly a safer assumption for lava flows than for sediments), the independence assumption should not be a serious problem.

The simplest idea would be to treat the dipole as just another part of the giant Gaussian distribution. This is completely incompatible with what is known of field component distributions from paleomagnetic data (Cox, 1970) in which the axial (*i.e.*, spin-axis-aligned) dipole has been dominant throughout geologic time (except during the brief periods of actual reversal). We therefore rule out this model.

The simplest modification of an entirely isotropic dipole model is one that ascribes to the dipole *variations*, the same statistical behavior as the non-dipole field, but, during times not associated with reversal, superimposes a steady axial part to account for the ascendancy of the g_1^0 term. This seems a reasonable approach given that the g_1^1 and h_1^1 terms also appeared to satisfy the giant Gaussian model for the non-dipole part of the field. Thus the statistical distribution for the g_1^0 term is envisioned as bimodal and symmetric, a combination of two normal distributions with centers at the present day value and its sign reversed counterpart. We take this opportunity to introduce some new terminology specifying the magnitude of the zonal terms of the geomagnetic field. Let $\gamma_l^0 = |g_l^0|$ for $l = 1, 2, \cdots$; then the statistical distribution for γ_1^0 will be closely approximated by a Gaussian distribution centered on $|g_1^0|$. (The standard deviation computed from the present-day spectrum for the dipole parts of the field is about 20% of the present axial dipole magnitude; thus the area under the normal pdf that is truncated by taking the absolute value will be very small.) Then at times not associated with reversal the magnetic field components may be written as

$$B_r' = B_r + f$$
$$B_\theta' = B_\theta + e$$
$$B_\phi' = B_\phi$$

where $f = 2\gamma_1^0 \sin\lambda$, $e = \gamma_1^0 \cos\lambda$ are the mean contributions at a site at latitude λ and, as we mentioned earlier, B_r, B_θ and B_ϕ, the random components, are Gaussian, zero mean and independent with variances derived from the spectrum at the core. We can compute the probability

density functions (pdfs) for the commonly measured elements of the geomagnetic field by per-
forming the necessary integrals. The techniques used for performing these calculations are laid
out in Appendix 2 for a general form for the axial dipole distribution. Numerical integration of
those pdfs yield cumulative distribution functions for comparison with the empirical cdfs
obtained for the data.

Figure 8 shows the resulting pdfs at a variety of latitudes for i and d, the modified inclina-
tion and declination. In these calculations we have simply set the mean of the magnitude of the
axial dipole to today's value ($\bar{\gamma}_1^0 = 30\mu T$). The distribution for i is skewed at mid and high lati-
tudes and the standard deviation is large at low latitudes. Figure 9 (solid line) is a plot of the
standard deviations and the bias as a function of latitude. (The bias is again the expected value
of i minus the axial dipole inclination for that latitude.) Note that even though everything
except the axial dipole part of the field had zero mean Gauss coefficients, this does not mean that
i or even I, the inclination, will average to the axial dipole value. This is fortunate, since there
exists a considerable body of paleomagnetic evidence in favor of biased inclinations (see *e.g.* Wil-
son, 1971; Merrill & McElhinny, 1983 Chapter 6). Also plotted on Figure 9, as symbols, are the
standard deviations and bias obtained for the global data compilation of Lee (1983), which were
plotted in Figure 5. It is evident that this model leaves something to be desired. The standard
deviations are all too high, although the variation with latitude has approximately the right
shape. The bias in the modified inclination changes sign at too high a latitude (again partly
reflecting the high standard deviation), and does not reach quite such low values in mid-latitudes
as it does for the data.

How closely should we expect the data to follow the model? The error bars in Figure 9 are
based on the assumption that the empirical distribution functions of Figure 4 represent the true
distribution functions for the secular variation. The effects of the inadequacy of this assumption
are hard to measure. Both the i and d data should have slightly higher standard deviations, $\sigma(i)$
and $\sigma(d)$, than predicted by the model because of the presence of errors in recording and measur-
ing the field. For the data, $\sigma(i)$ will also be biased towards high values because inclinations from

a range of latitudes with slightly differing means are combined to provide a single empirical distribution for that latitude band. The only mechanism by which the data standard deviation could be lower than that for the model is if there are insufficient data to sample the complete range of directions possible for the secular variation. As noted in the section on paleodata, the data of Figure 7 suggests that this is only influencing one or two of the standard deviation points of Figure 5. These are again marked by asterisks in Figure 9. The net result of the above possible sources of bias is that, on the whole we should expect $\sigma(i)$ and $\sigma(d)$ for the model to lie slightly below those obtained for the data, except possibly for the data represented by the asterisks.

From Figure 9 we must conclude that this simplest model does not satisfy the data. We look now for the least departure from the isotropic Gaussian model with non-zero axial dipole, that is consistent with the data. In order to do this it is worth restating the assumptions for this model and looking at whether it is possible to vary any of the basic parameters. The fundamental assumption is that the spatial statistics of the present-day field are typical of the paleofield and may be used to determine the variance, α^2, for the scaled Gauss coefficients of the non-dipole part of the field and also the non-axial parts of the dipole field. The magnitude of the axial part of the dipole field is also taken to be Gaussian, with the same variance, and a mean value given by the present day value for g_1^0. There are three parameters that can be varied;

    1) α is computed from the present day field, and will depend on the level in the Earth at which the spectrum is assumed to be white,

    2) $\bar{\gamma}_1^0$ the mean value for the axial dipole magnitude may not be the same as the present day value, and

    3) the variance for the dipole components of the field may be different from that for the non-dipole part.

Since we have only directional data, varying α or $\bar{\gamma}_1^0$ will have the same effect, an increase in $\bar{\gamma}_1^0$ corresponding to a decrease in α. Figure 10 shows the effect of varying $\bar{\gamma}_1^0$ on the model curves for B{i}, $\sigma(i)$ and $\sigma(d)$ as a function of latitude. Here the parameters have been normalized so that $\bar{\gamma}_1^0 = 1.0$ corresponds to the present day field value of $30\mu T$. In Figure 11 model curves are

plotted for various values of σ_1, the standard deviation in each of the Gauss coefficients for the dipole part of the field (*i.e.*, γ_1^0, g_1^1 and h_1^1). σ_1 is normalized in units of $\bar{\gamma}_1^0$, so that the giant Gaussian model whose pdfs are plotted in Figure 8 has $\sigma_1 = 0.207$ as determined from the spectrum of Figure 1. It is readily seen that in order to make the model parameters $\sigma(i)$ and $\sigma(d)$ approximate those for the data we must either increase $\bar{\gamma}_1^0$ (or equivalently decrease α) or decrease σ_1. This also makes the zero crossing for B{i} closer to the right latitude, but makes the bias insufficiently negative at mid to high latitudes. There is little difference in the shapes of the curves obtained by varying these parameters, and the data is certainly not of good enough quality to enable us to pick between them. We must therefore look to other data to constrain these parameters.

The variance of the scaled Gauss coefficients, and from these the variances in the field coefficients (see Section 1 and Appendix 2), are determined from the spectrum. Increasing the depth at which the spectrum appears white, results in an increase in α and therefore a worse fit to the data. There is no evidence to suggest that the spectrum is white at a radius greater than the core-mantle boundary (in fact a number of authors have suggested it lies below there, *e.g.*, Langel & Estes, 1982, find a level of $0.52a$ and $\alpha = 36.7\mu T$, which results in a substantial increase in the variance in the field components). A decrease in the value of α is therefore not consistent with the known properties of the present field.

Another source of information is the available paleomagnetic intensity data. McFadden & McElhinny (1982) have compiled the available data for the past 5Ma (with VGP latitudes of greater than 45°), and performed a statistical analysis of their virtual dipole moments (VDMs). The VDM is the equivalent dipole moment which would have produced the measured intensity at the calculated paleolatitude (assuming a dipolar field) of the sample. Working with VDMs enables these authors to combine data from sites at different latitudes. Unfortunately , there is no means of separating the g_1^0 component of the intensity from the non-axial dipole and non-dipole parts of the field. However, by taking random samples of the present day field, McElhinny & Senanayake (1982) concluded that the scatter in VDMs due to non-dipole components was

Gaussian with standard deviations ranging between 12.5 and 20.7% of the mean. McFadden & McElhinny (1982) find a model for the VDMs consisting of nested distributions due to paleointensity errors, variation in the non-dipole parts of the field and a true dipole moment distribution. Their estimate for the preferred value of the true dipole moment corresponds to the peak (or mode) of the truncated Gaussian distribution used to model the true dipole moment, and is $8.67 \pm 0.65 \times 10^{22}$ A m^2 (to within the 95% confidence limit). This corresponds quite closely to the value of 9.07×10^{22} A m^2, that they obtained from the arithmetic mean of the observed VDMs.

The dipole moment p is related to the Gauss coefficients of degree 1 by

$$p = \frac{4\pi a^3}{\mu_0} \left[(g_1^0)^2 + (g_1^1)^2 + (h_1^1)^2 \right]^{1/2}$$

For the present day field $p = 7.91 \times 10^{22}$ A m^2. If the g_1^1 and h_1^1 terms are indeed Gaussian with zero mean, then their combined contribution to the true dipole moment will be that due to their scatter about the mean. Assuming, as before, that the present day field is typical, we can compare today's dipole moment with McFadden & McElhinny's estimate of the true dipole moment to see whether g_1^0 for the present day differs drastically from $\bar{\gamma}_1^0$ for the past 5Ma. The difference of about 10% suggests that this is not the case. We might be justified in increasing $\bar{\gamma}_1^0$ by 10%, but hardly any more. Since the discussion above suggests that α is if anything underestimated (which would counteract the increase in $\bar{\gamma}_1^0$) we choose to leave it unaltered. Figure 10 clearly shows that a 10% change in the value of $\bar{\gamma}_1^0$ will not significantly improve the fit to the data. An increase of about 50% would be required in order to reduce the standard deviations in i and d to about the right level. This is completely inconsistent with what is known from both the paleointensity data and the constraints on the present day geomagnetic spectrum.

The constraints on σ_1 are much less rigorous. These come entirely from the present day field values. Our Gaussian model for the field assumes that the scaled dipole coefficients γ_1^0, g_1^1 and h_1^1, are drawn from the same distribution as the rest of the coefficients (except that γ_1^0 has a non-zero mean). Support for this is based on the fact that g_1^1 and h_1^1 do not alter the Kolmogorov-Smirnov test for normality, when they are included in the distribution. However,

this may simply be chance; there are only two data involved, and there is considerable evidence for believing that the dipole part of the field is special. Why else would it dominate the non-dipole part so much of the time? Figure 11 shows that a value for σ_1 of 0.1 would provide a much more acceptable fit to the standard deviation data, than $\sigma_1 = 0.207$ obtained from the spectrum. The present day values of $g_1^1 = 0.0650 g_1^0$ and $h_1^1 = 0.1878 g_1^0$ are entirely consistent with this, as both samples from the distribution lie within 2 standard deviations of the zero mean. Decreasing σ_1 still further (e.g. to 0.05, as shown in Figure 11) would enable us to constrain all the standard deviation data for the model to lie below those of the paleomagnetic data. However, this stretches the limits of what is plausible for the present day field, as it would require the present day sample of h_1^1 to lie at $3.764 \sigma_1$ in the distribution. In a random sample from a Gaussian distribution this has a probability of less than one part in ten thousand of occurring, hardly what one would expect from a typical sample of the field.

Reduction of the variance in the directional data, has been obtained at the expense of almost eliminating the bias in i. The zero crossing now occurs at about the right latitude, but the large negative values at mid-latitudes cannot be obtained from a dipole field with such low variance. A different means of generating distributions with a significant bias in i is to include a zonal quadrupole term with a non-zero mean magnitude.

The idea that the time averaged geomagnetic dipole does not correspond to that of a geocentric axial dipole (GAD) is not a new one: many paleomagnetists have proposed it (see e.g., Wilson, 1971; Creer, Georgi & Lowrie, 1973; Wells, 1973; Georgi, 1974; Wilson & McElhinny, 1974; Merrill & McElhinny, 1977; Coupland & Van der Voo, 1980; Livermore, Vine & Smith, 1983, 1984). Many of these authors have performed least squares fits for the spherical harmonic coefficients using paleopole data drawn from sites around the world. The resulting models may be rather strongly influenced by data distribution, whether non-zonal terms are included, and the degree to which the spherical harmonic expansion is carried. However, there appears to be a general consensus that for the past 5Ma the inclusion of a g_2^0 term offers a significant improvement over the GAD in fitting the available data. Livermore, Vine & Smith (1983) give a value of

$\overline{\gamma}_2^0 = .05\overline{\gamma}_1^0$, in agreement with that obtained by Merrill & McElhinny (1977). They also suggest that a value of $\overline{\gamma}_3^0 = .02\overline{\gamma}_1^0$ might be added for the last 5Ma, (although this could be due in part to data errors), and that h_2^1 may be significant in the average field for 0-5Ma. These results are substantially in agreement with a study of inclination anomalies by Lee & McElhinny (unpublished, but cited in Merrill & McElhinny (1983)), except that they suggest that the $\overline{g}_2^0$ has a reversing and non-reversing part. Lee & McElhinny also looked at the average values of g_1^1 and h_1^1 and found no evidence to indicate that they are significantly different from zero. They did not look at second order non-zonal terms in their analysis.

Figure 12 shows the effect on the now familiar model parameters of varying $\overline{\gamma}_2^0$, the mean of the magnitude of g_2^0. All of these models have $\overline{\gamma}_1^0 = 1.0$ and $\sigma_1 = 0.1$, as the evidence cited above suggests that these are reasonable values for these parameters. It is assumed also that $\overline{g}_2^0$ is of the same sign as and reverses sign with $\overline{g}_1^0$. This is consistent with the paleomagnetic evidence that the inclination bias is negative for both normal and reverse fields (see *e.g.*, Merrill & McElhinny, 1983, p.185 figure 6.7). The best fit to the data of Lee (1983) is obtained with $\overline{\gamma}_2^0 \cong .06$ and is shown in Figure 13. Since our data set is somewhat sparse for our goal of determining the actual pdfs for directions at any given latitude, we mapped all the southern hemisphere data onto the upper hemisphere. Our modeling will therefore not indicate the necessity for a significant $\overline{\gamma}_3^0$ component, although it would be a simple matter to include such a term if it were necessary, and we had the data resolution to detect it. Similarly, we have made no attempt to include non-zonal components with non-zero mean in our model, because it is expected that by averaging data around latitude bands and over the 5Ma time interval non-zonal effects will average out.

Figures 14 and 15 compare the cdfs for the preferred model (with $\overline{\gamma}_1^0 = 1.0$, $\sigma_1 = 0.1$ and $\overline{\gamma}_2^0 = .06$) with the data distribution functions of Figure 6. Here, the solid lines represent the average data cdfs over the latitude bands (0—15°, 15—30°, 30—45° and 45—70°) and the finely dashed lines give the model cdfs for the boundaries of the latitude strips. These should represent bounds

between which the data lie, provided the data are sufficiently good and the model is an adequate description of the statistics. For the modified inclination (Figure 14) the average model expected from combining data at the given sites is computed and is given by the heavy dashed line. It agrees well with the empirical cdfs, except in the 0—15° strip for which either a larger quadrupole term or a lower dipole standard deviation would improve the fit somewhat. The declination data (Figure 15), as might be expected does somewhat less well. This is mostly because in both the 15—30° and 45—70° strips the declinations are biased towards positive values. This could be due to bias arising from insufficient averaging in longitude in the sites used. Right handedness of VGP positions was also noted by Wilson (1972) and others since then. Lee (1983) finds no evidence for believing the time averaged g_1^1 and h_1^1 terms significantly different from zero, when all the sources of error in the data are taken into account.

3. Conclusions

In this study an attempt has been made to find a simple statistical model for the Gauss coefficients to describe the secular variation of the geomagnetic field. Working with the Gauss coefficients, instead of the directional data enables us to find a model that can simultaneously satisfy all the statistical requirements imposed by the vector field variation. Using the spatial spectrum of the present day field it is possible to derive a statistical model for the non-dipole part of the field. A comparison of the computed probability distribution functions for the modified inclination and declination data with paleomagnetic data spanning the past 5Ma indicates a number of features about the geomagnetic field statistics. (1) With the exception of the axial dipole and axial quadrupole terms each Gauss coefficient may be regarded as independently normally distributed with zero mean and a standard deviation for the non-dipole terms consistent with a white source at the core surface. (2) The dipole part of the field cannot have the same statistical distribution as the non-dipole part. The axial dipole has predominated and both the non-axial parts of the dipole and the magnitude of the axial part of the dipole have lower variance (by about a factor of 4) than if they belonged to the same giant Gaussian distribution as the non-dipole part of the field. (3) The hypothesis based on the present day field that all the non-dipole

Gauss coefficients have zero mean is inconsistent with the paleodata. Although the inclination measurements are biased towards low values (relative to the GAD hypothesis) by the statistical variation in the Gauss coefficients, this bias alone is not sufficient to account for the inclination anomalies found in the paleodata; a quadrupole term with non-zero mean magnitude is required. A value of $\bar{\gamma}_2^0 = .06\bar{\gamma}_1^0$ for the past 5Ma provided a reasonably good fit to the paleodata; this agrees with typical values found by other workers (Livermore, Vine & Smith, 1983; Lee, 1983).

The statistical distributions for the first 3 degree spherical harmonic coefficients are plotted in Figure 16 for this model. Note the quite narrow distribution of g_1^0 about its peak normal and reversed values, and how the variance drops off rapidly with increasing degree. The g_2^0 distribution results from the sum of two normal distributions, centered at $\pm .06\bar{g}_1^0$. There is an implicit covariance between $\bar{g}_2^0$ and $\bar{g}_1^0$, in that they are required to always have the same sign. Table 1 lists some parameters associated with this model. This simple model for the Gauss coefficients also enables us to compute the expected probability density functions for the conventional field directions D and I at any latitude (Figure 17). The model is a complete description of the geomagnetic field in the sense that it is capable of predicting the expected statistics of any measurable feature of the field. For example, we could straightforwardly compute distribution functions for intensity measurements anywhere on the Earth; there is no decoupling of intensity and directional data in the spherical harmonic representation, making the model eminently testable by any or all of the available data.

Some remaining questions clearly require further work. This study is based on a very limited data set of combined sedimentary and lava flow measurements. Information from lava flows is usually more suitable for statistical studies of secular variation, because there is less smoothing inherent in the recording process. A better data set requires finding all the available lava flow data for which individual flow mean values have been published and using these to obtain the empirical cdfs for a data set. This would require an extensive literature search since (to our knowledge) there is no existing compilation of such data (the published pole lists generally contain means from several sites rather than flow means for a given study). It remains unclear what

criteria should be used in selecting these data; internal consistency as represented by α_{95} is clearly required, but it seems desirable not to exclude transitional data corresponding to low VGP latitudes, since these transitional fields are after all part of the secular variation. However, if all these data are included, we then encounter problems such as described in this paper with the Icelandic data which appear to have too many transitional flows. This probably reflects the combination of sampling two erratic processes, namely the reversal of the magnetic field and the volcanic eruptions that generate the flows. A larger data set can only improve the situation.

The acquisition of a large global data set could provide us with more accurate cdfs for i and d. This study has shown that it is possible to satisfy the data with a model of the type discussed. A better data set could give better estimates for the parameters of the model, perhaps justifying setting up a formal inversion procedure.

Acknowledgments

Appendix 1: Spherical Harmonic Representation of the Geomagnetic Field

The method of analysis for global geomagnetic data was devised in 1838 by Gauss and involves representing the geomagnetic field of internal origin as the gradient of a potential Ψ whose spatial variation is specified by an infinite sum of spherical harmonics.

$$\Psi = a \sum_{l=1}^{\infty} \sum_{m=0}^{l} (\frac{a}{r})^{l+1} (g_l^m \cos m\phi + h_l^m \sin m\phi) P_l^m(\cos\theta)$$

$$\vec{B} = -\nabla\Psi$$

i.e.,

$$B_\theta = -\frac{1}{r}\frac{\partial\Psi}{\partial\theta} \quad B_\phi = -\frac{1}{r\sin\theta}\frac{\partial\Psi}{\partial\phi} \quad B_r = -\frac{\partial\Psi}{\partial r}$$

where g_l^m and h_l^m are known as the Schmidt partially normalised Gauss coefficients, r, θ and ϕ are the usual spherical coordinates, and P_l^m are the partially normalised Schmidt functions related to the associated Legendre polynomials, P_{lm}, (Abramowitz & Stegun, 1965) by

$$P_l^m = P_{lm} \quad \text{for} \quad m=0$$

$$P_l^m = \left| \frac{2(l-m)!}{(l+m)!} \right|^{\frac{1}{2}} P_{lm} \quad \text{for} \quad m>0$$

The term "partial normalization" arises from the fact that within each degree l the average value of the square of P_l^m over the surface of the sphere has the same value for all values of m, i.e.

$$\int_0^{2\pi} d\phi \int_{-1}^{1} d(\cos\theta) P_l^m(\cos\theta) \begin{Bmatrix} \cos m\phi \\ \sin m\phi \end{Bmatrix} P_l^{m'}(\cos\theta) \begin{Bmatrix} \cos m'\phi \\ \sin m'\phi \end{Bmatrix} = \frac{4\pi}{2l+1}\delta_{ll'}\delta_{mm'}$$

The Gauss coefficients are commonly used to describe the field, since they are sufficient to determine the field model at any point on the Earth's surface. Successively higher degree and order terms correspond to components of the field with greater spatial variability; eg, g_1^0 is the coefficient of the axial dipole term, g_2^0 the axial quadrupole, etc. The zonal terms $(m=0)$ exhibit latitudinal spatial variation, and the non-zonal terms longitudinal variation. A more convenient mathematical representation of the field is in terms of the fully normalised complex spherical harmonics, $Y_l^m(\theta,\phi)$, with complex coefficients b_l^m

$$\Psi = a \sum_{l=0}^{\infty} \sum_{m=-l}^{l} \left(\frac{a}{r}\right)^{l+1} b_l^m Y_l^m(\theta,\phi)$$

The fully normalised spherical harmonics Y_l^m are related to the associated Legendre polynomials $P_{lm}(\cos\theta)$ by

$$Y_l^m(\theta,\phi) = \sqrt{\frac{2l+1}{4\pi} \frac{(l-m)!}{(l+m)!}} P_{lm}(\cos\theta) e^{im\phi}$$

and

$$\int_0^{2\pi} d\phi \int_{-1}^{1} d(\cos\theta) Y_{l'}^{m'*}(\theta,\phi) Y_l^m(\theta,\phi) = \delta_{ll'} \delta_{mm'}$$

Although the Schmidt normalization is commonly used in geomagnetism, we will use this fully normalised representation where it simplifies the mathematics (see Appendix 2). The fully normalised b_l^m may be related to the Schmidt coefficients by

$$b_l^m = \begin{cases} (-1)^m \sqrt{\dfrac{2\pi}{2l+1}} [g_l^m - ih_l^m] & m > 0 \\[2ex] \sqrt{\dfrac{4\pi}{2l+1}} g_l^0 & m = 0 \\[2ex] (-1)^m (b_l^m)^* & m < 0 \end{cases}$$

The Gauss coefficients are usually determined up to some finite degree by performing a least squares fit to the available field data (Langel, 1985, provides a review of methods and models). Downward continuation of these models enables us to make estimates of what the field looks like on the core-mantle boundary. Spherical harmonic fits can be highly susceptible to poor data distribution, and this problem is exacerbated by downward continuation of the models. Shure, Parker and Backus (1982) developed a technique for finding the smoothest model, in a certain specified sense, that is consistent with the data. These models, known as harmonic spline models, to a large degree compensate for poor data distribution, by suppressing spatial variation in the field that is not required by the data.

Appendix 2: Computation of Variances and Covariances for B_r, B_θ, and B_ϕ.

As indicated in the previous section let us suppose that g_l^m and h_l^m are independent, normal random variables of zero mean for $l \geq 2$. Then g_l^m and h_l^m satisfy the following

$$E[g_l^m] = E[h_l^m] = 0$$

$$E[g_l^m g_l^{m'}] = E[h_l^m h_l^{m'}] = \sigma_l^2 \delta_{ll'} \delta_{mm'}$$

$$E[g_l^m h_l^{m'}] = 0 \qquad \text{for all } l, l', m, m'$$

where σ_l^2 is the variance of the normal distribution associated with degree l. First let us derive the variance of the non dipole part of the field components B_r, B_θ, B_ϕ. This is facilitated by using the fully normalised spherical harmonic representation for the potential. Making use of the relationships between the b_l^m and the Schmidt coefficients, we find

$$E[b_l^m (b_l^m)^*] = \frac{2\pi}{2l+1} E[(g_l^m)^2 + (h_l^m)^2] \quad m \neq 0$$
$$= \frac{4\pi}{2l+1} \sigma_l^2$$

$$E[b_l^0 (b_l^0)^*] = \frac{4\pi}{2l+1} E[(g_l^0)^2]$$
$$= \frac{4\pi}{2l+1} \sigma_l^2$$

Thus $E[b_l^m (b_l^m)^*]$ is the same regardless of whether or not $m = 0$. Because $E[g_l^m h_l^{m'}] = 0$ for $l = l'$ or $m = m'$ the only non-zero terms possibly remaining are of the form $(m \neq 0)$,

$$E[b_l^m (b_l^{-m})^*]$$

when g_l^m and h_l^m appear in both complex numbers.

$$E[b_l^m (b_l^{-m})^*] = (-1)^m \frac{2\pi}{2l+1} E[(g_l^m)^2 - (h_l^m)^2 - 2i g_l^m h_l^m]$$
$$= 0$$

We make use of the above expressions in deriving the field component variances and covariances. In addition it is useful to remember the Spherical Harmonic Addition Theorem (Jackson 1963, p.67):

$$\frac{2l+1}{4\pi} P_l(\hat{r}_0 \cdot \hat{r}) = \sum_{m=-l}^{l} Y_l^m(\theta_0, \phi_0) Y_l^m(\theta, \phi)^*$$

Letting $\hat{r} = \hat{r}_0$ yields

$$\sum_{m=-l}^{l} |Y_l^m(\theta, \phi)|^2 = \frac{2l+1}{4\pi}$$

Differentiating this equation yields some further sums which are useful. $\frac{\partial}{\partial\theta}$ yields

$$\sum_{m=-l}^{l} Y_l^m(\theta,\phi)^* \frac{\partial Y_l^m}{\partial\theta} = 0$$

Some further manipulation and differentiation of the addition theorem yields

$$\sum_{m=-l}^{l} |\frac{\partial Y_l^{m*}}{\partial\theta}|^2 = \frac{l(l+1)(2l+1)}{8\pi}$$

We start with the radial field. From our non-dipole field model $E[B_r]=0$. Thus

$$
\begin{aligned}
\text{var}[B_r] &= E[B_r B_r^{*}] \\
&= \sum_l \sum_{l'} \sum_m \sum_{m'} (l+1)(l'+1) Y_l^m (Y_{l'}^{m'}) E[b_l^m b_{l'}^{m'*}] \\
&= \sum_l (l+1)^2 \frac{4\pi\sigma_l^2}{2l+1} \sum_m |Y_l^m|^2 \\
&= \sum_{l=2}^{\infty} (l+1)^2 (\frac{c}{a})^{2l} \frac{4\pi\alpha^2}{(l+1)(2l+1)^2} \frac{2l+1}{4\pi} \\
&= \alpha^2 \sum_{l=2}^{\infty} \frac{l+1}{2l+1} (\frac{c}{a})^{2l} \\
&= \alpha^2 [\tfrac{1}{4}(1-\frac{c^2}{a^2})^{-1} + \tfrac{1}{4}(\frac{a}{c}) \text{th}^{-1}(\frac{c}{a}) - 1 - \frac{2}{3}\frac{c^2}{a^2}] \\
&= .0753\alpha^2 = (7.60)^2 \, (\mu T)^2
\end{aligned}
$$

Similarly $E[B_\theta]=0$ and

$$
\begin{aligned}
\text{var}[B_\theta] &= \sum_l \frac{4\pi\sigma_l^2}{2l+1} \sum_m |\frac{\partial Y_l^m}{\partial\theta}|^2 \\
&= \sum_{l=2}^{\infty} (\frac{c}{a})^{2l} \frac{4\pi\alpha^2}{(2l+1)^2(l+1)} \frac{l(l+1)(2l+1)}{8\pi} \\
&= \frac{\alpha^2}{2} \sum_{l=2}^{\infty} \frac{l}{(2l+1)} (\frac{c}{a})^{2l} \\
&= .0262\alpha^2 = (4.48)^2 (\mu T)^2
\end{aligned}
$$

Symmetry arguments clearly dictate that $E[B_\phi]=0$ and $\text{var}[B_\phi] = \text{var}[B_\theta]$.

Since B_r, B_θ and B_ϕ are derived from sums of Gaussian random variables, they are clearly Gaussian also. Their covariances may be readily computed from

$$\text{cov}[B_r, B_\theta] = E[B_r B_\theta^{*}] = \sum_l \sum_{l'} \sum_m \sum_{m'} (l+1) Y_l^m (\frac{\partial Y_{l'}^{m'}}{\partial \theta})^{*} E[b_l^m b_{l'}^{m'*}]$$

$$= \sum_{l=2}^{\infty} (l+1) \frac{4\pi\sigma_l^2}{2l+1} \sum_{m=-l}^{l} Y_l^m (\frac{\partial Y_l^m}{\partial \theta})^{*}$$

$$= 0$$

Clearly by symmetry $E[B_r B_\phi^{*}]=0$ and similarly for $E[B_\theta B_\phi^{*}]$. Thus the non-dipole field components B_r, B_θ and B_ϕ are independent Gaussian variables with zero mean and standard deviations which are equal for the two horizontal components and larger for the radial component.

Appendix 3: Computation of the Distribution Functions for Declination and Inclination

Let us suppose that the pdf for the axial part of the dipole field, f_D may be written as a sum of Gaussian kernel functions, $G_j(x)$, centered at positions X_j

$$f_D(x) = \sum_j c_j G_j(x)$$

where

$$G_j(x) = \exp-\frac{1}{2}\left\{ \frac{(x-X_j)}{h_j} \right\}^2$$

and

$$\sum_j c_j h_j = \frac{1}{\sqrt{2\pi}} \qquad c_j = \exp\{\alpha_j\} \geq 0$$

This is a conventional technique of representing empirically an unknown pdf (see *e.g.*, Silverman, 1986); $f_D(x)$ is known as a kernel estimator. We will assume that X_j, the locations of the kernels, and h_j, their widths, are chosen *a priori* and $h_j = h = $ constant. Then the axial dipole contribution to the field components B_r and B_0 at any given site is distributed as

$$f_D(x') = \sum_j \frac{c_j}{k_i} \exp-\frac{1}{2}\left\{ \frac{(x'-X_j')}{k_i h_j} \right\}^2$$

where

$$x' = k_i x \quad \text{and} \quad k_i = \cos\lambda \quad \text{for } B_\theta$$

$$X_j' = k_i X_j \quad \text{and} \quad k_i = \sin\lambda \quad \text{for } B_r$$

λ is the latitude at the site in question.

In its simplest form (as is used in this work) $f_D(x)$ is just the sum of two Gaussian distributions, one centered on the value of the present day normal field, and the other on the reverse field (see the distribution function for g_1^0 in Figure 16). Then if, as discussed in Section 1, the non-dipole part of the field has a Gaussian distribution, $f_{ND}(y)$, that is independent of the dipole part of the field, the cumulative distribution function for the field components B_r and B_θ may be computed from

$$Pr(B_i \leq \beta) = \iint_S f_D(x')f_{ND}(y)dx'dy$$

$$f_{ND}(y) = \frac{1}{\sqrt{2\pi}\sigma_i}\exp-\tfrac{1}{2}\left\{\frac{y}{\sigma_i}\right\}^2, \qquad \sigma_i = \sigma_\theta, \sigma_r, \sigma_\phi$$

where S is the region satisfying $x' + y \leq \beta$, and f_{ND} includes the g_1^1 and h_1^1 random variation. Then $f(\beta)$ the probability density function for the field component will be

$$f(\beta) = \frac{d}{d\beta} Pr(B_i \leq \beta)$$

and will again be a sum of Gaussians

$$f(\beta) = \sum_j \frac{c_j h}{(\sigma_i^2 + k_i^2 h^2)^{1/2}}\exp-\frac{1}{2}\left\{\frac{(\beta - X_j')^2}{(\sigma_i^2 + k_i^2 h^2)}\right\}$$

Note that this is easily modified to include a non-zero mean for the g_2^0 (and or any other higher order) term in the non-dipole distribution function.

Now to compute the distribution function for $\tan I$ we need first to find that for $H = (B_\theta^2 + B_\phi^2)^{1/2}$. Letting

$$B_\theta = l\cos\theta \qquad B_\phi = l\sin\theta$$

and

$$Y_j = k_\theta X_j = X_j \cos\lambda$$

we have

$$Pr(H \le l) = \sum_j \frac{c_j h}{(\sigma_\theta^2 + k_\theta^2 h^2)^{1/2}} \int_0^l \int_0^{2\pi} \frac{l \, dl \, d\theta}{\sqrt{2\pi}\sigma_\phi} \exp-\frac{1}{2}\left\{ \frac{l^2\sin^2\theta}{\sigma_\phi^2} - \frac{(l\cos\theta - Y_j)^2}{(\sigma_\theta^2 + k_\theta^2 h^2)} \right\}$$

or for the pdf for H

$$f_H(l) = \sum_j \frac{c_j h}{\sqrt{2\pi}\sigma_\phi(\sigma_\theta^2 + k_\theta^2 h^2)^{1/2}} \int_0^{2\pi} l \, d\theta \exp-\frac{1}{2}\left\{ \frac{l^2\sin^2\theta}{\sigma_\phi^2} - \frac{(l\cos\theta - Y_j)^2}{(\sigma_\theta^2 + k_\theta^2 h^2)} \right\}$$

The pdf for $t = \tan I$ is given by

$$f_{\tan I}(t) = \int_0^\infty l \, dl f_r(tl) f_H(l)$$

where $f_r(tl)$ is the pdf for the radial component of the field at $R = H \tan I$, i.e.,

$$f_r(tl) = \sum_j \frac{c_j h}{(\sigma_r^2 + k_r^2 h^2)^{1/2}} \exp-\frac{1}{2}\left\{ \frac{(lt - Z_j')^2}{(\sigma_r^2 + k_r^2 h^2)} \right\}$$

and $Z_j = k_r X_j = 2X_j \sin\lambda$

Some algebraic manipulation yields

$$f_{\tan I} = C \sum_n c_n \sum_j c_j \exp(-\tau) \int_0^{2\pi} d\theta \left(\frac{\pi}{2\alpha^3} \right)^{1/2} \exp\left(\frac{\beta^2}{\alpha}\right) \text{erfc}\left(-\frac{\beta}{\sqrt{\alpha}}\right) \left[\frac{\beta^2}{\alpha} + \frac{1}{2} \right] + \frac{\beta}{2\alpha^2}$$

with

$$\alpha = \alpha(\theta) = \frac{fg\sin^2\theta + eg\cos^2\theta + eft^2}{efg}$$

$$\beta = \beta(\theta) = \frac{g\cos\theta \, Y_j + ftZ_n}{fg}$$

$$\tau = \frac{gY_j^2 + fZ_n^2}{fg}$$

$$e = 2\sigma_\phi^2$$

$$f = 2(\sigma_\theta^2 + k_\theta^2 h^2)$$

$$g = 2(\sigma_r^2 + k_r^2 h^2)$$

$$C = \frac{h^2}{\sqrt{2\pi}\sigma_\phi(\sigma_\theta^2 + k_\theta^2 h^2)^{1/4}}$$

The θ integral can be computed rapidly using the trapezoidal rule. The inclination pdf is then

$$f_I(i) = \sec^2 i \, f_{\tan I}(t)$$

Similarly the declination distribution may be computed from

$$Pr(d \leq \delta) = \sum_j \frac{c_j h}{\sqrt{2\pi}\sigma_\phi(\sigma_\theta^2 + k_\theta^2 h^2)^{1/4}} \int_0^\delta \int_0^\infty l dl d\theta \exp{-\frac{1}{2}\left\{\frac{l^2 \sin^2\theta}{\sigma_\phi^2} - \frac{(l\cos\theta - Y_j)^2}{(\sigma_\theta^2 + k_\theta^2 h^2)}\right\}}$$

and

$$f_D(\theta) = \sum_j \frac{c_j h}{\sqrt{2\pi}\sigma_\phi(\sigma_\theta^2 + k_\theta^2 h^2)^{1/4}} \int_0^\infty l dl \exp{-\frac{1}{2}\left\{\frac{l^2 \sin^2\theta}{\sigma_\phi^2} - \frac{(l\cos\theta - Y_j)^2}{(\sigma_\theta^2 + k_\theta^2 h^2)}\right\}}$$

$$= \sum_j \frac{c_j h}{\sqrt{2\pi}\sigma_\phi(\sigma_\theta^2 + k_\theta^2 h^2)^{1/4}} \exp(\frac{v^2}{\mu} - \rho) \left[\left(\frac{\pi v}{4\mu^3}\right)^{1/2} \mathrm{erfc}(-\frac{v}{\sqrt{\mu}}) + \frac{1}{2\mu}\exp(-\frac{v^2}{\mu})\right]$$

with

$$\mu = \mu(\theta) = \frac{\sin^2\theta(\sigma_\theta^2 + k_\theta^2 h^2) + \cos^2\theta\sigma_\phi^2}{2\sigma_\phi^2(\sigma_\theta^2 + k_\theta^2)}$$

$$v = v(\theta) = \frac{\cos\theta Y_j}{2(\sigma_\theta^2 + k_\theta^2 h^2)}$$

$$\rho = \frac{Y_j^2}{2(\sigma_\theta^2 + k_\theta^2 h^2)}$$

$\mathrm{erfc}(x)$ is the complete error function (Abramowitz & Stegun, 1965, p.299)

The pdfs for I and D are readily converted to those for the modified field directions i and d. Comparison with the data requires cdfs for d and i. These are obtained by using a cubic spline quadrature scheme to integrate the numerical values of the pdfs obtained on a uniform grid for d

and i. Obtaining the cdfs also provides some reassurance about the accuracy of the above results, since we can check that they integrate to unity.

References

Abramowitz, M., & Stegun, I.A., (1965) *Handbook of Mathematical Functions,* Dover, New York.

Baag, C. & Helsley, C.E. (1974), Geomagnetic secular variation model E, *J. Geophys. Res., 79, 4918–4922.*

Bullard, E.C., Freedman, C., Gellman, H., & Nixon, J. (1950), The westward drift of the earth's magnetic field; *Phil. Trans. Roy. Soc., A, 243, 67–92.*

Clement, B. M., & Kent, D.V. (1984), Latitudinal dependence of geomagnetic polarity durations, *Nature, 310, 488–491.*

Clement, B. M., & Kent, D.V. (1984), A detailed record of the Lower Jaramillo polarity transition from a southern hemisphere, deep-sea sediment core, *J. Geophys. Res., 89, 1049–1058.*

Coupland, D.H., & Van der Voo, R., (1980) Long term nondipole components in the geomagnetic field during the last 130 M.Y., *J. Geophys. Res., 85, 3529-3548.*

Cox, A. (1962), Analysis of the present geomagnetic field for comparison with paleomagnetic results, *J. Geomag. Geoelectr., 13, 101–112.*

Cox, A. (1970), Latitude dependence of the angular dispersion of the geomagnetic field; *Geophys. J. Roy. Astron. Soc., 20, 253– 269.*

Creer, K.M. (1962), The dispersion of the geomagnetic field due to secular variation and its determination for remate times from paleomagnetic data, *J. Geophys. Res., 67, 3461–3476.*

Creer, K.M., Irving, E., & Nairn, A.E.M. (1959), Paleomagnetism of the Great Whin Sill, *Geophys. J. Roy. Astron. Soc., 2, 306–323.*

Creer, K.M., Georgi, D.T., & Lowrie, W., (1973) On the representation of the Quaternary and late Tertiary geomagnetic field in terms of dipoles and quadrupoles, *Geophys. J. Roy. astr. Soc., 33, 323-345.*

Doell, R.R. (1969), Paleomagnetism of the Kau Volcanic Series, Hawaii; *J. Geophys. Res., 74, 4857–4868.*

Doell, R.R. (1972a), Paleomagnetism of lava flows from Kauai, Hawaii; *J. Geophys. Res., 77, 862–876.*

Doell, R.R. (1972b), Paleosecular variation of the Honolulu Volcanic Series, Oahu, Hawaii; *J. Geophys. Res., 77, 2129–2138.*

Doell, R.R. (1972c), Paleomagnetism of volcanic rocks from Niihau, Nihoa and Necker Islands, Hawaii; *J. Geophys. Res., 77, 3725–3730.*

Doell, R.R., & Cox, A. (1965), Paleomagnetism of Hawaiian lava flows; *J. Geophys. Res., 70, 3377–3405.*

Doell, R.R., & Dalrymple, B. (1973), Potassium argon ages and paleomagnetism of the Waianae and Koolau Volcanic Series, Oahu, Hawaii; *Geol. Soc. Amer. Bull., 84, 1217–1242.*

Eckhardt, D.H. (1984), Correlations between global features of terrestrial fields, *Mathematical Geology, 16, 155-171.*

Efron, B., & Tibshirani, R. (1986), Bootstrap methods for standard errors, confidence intervals, and other measures of statistical accuracy, *Statistical Science, 1, 54-77.*

Fisher, R.A., (1953) Dispersion on a sphere, *Proc. Roy. Soc. A 217, 295-305.*

Georgi, D.T., (1974) Spherical harmonic analysis of paleomagnetic inclination data, *Geophys. J. Roy. astr. Soc., 39, 71-86.*

Gubbins, D. (1983), Geomagnetic field analysis - I. Stochastic inversion. *Geophys. J. Roy. astr. Soc., 73, 641-652.*

Harrison, C.G.A. (1980), Secular variation and excursion of the earth's magnetic field, *J. Geophys. Res., 85, 3511–3522.*

Irving, E., & Ward, M.A. (1964), A statistical model of the geomagnetic field, *Pure Appl. Geophys., 57, 47–52.*

Kendall, M., & Stuart, A. (1979), *The Advanced Theory of Statistics, Vol. 2, Inference and Relationship, 4th edition,* MacMillan, New York.

Jackson, J.D., (1963) *Classical Electrodynamics,* Wiley, New York.

Kent, D. V., & Opdyke, N.D., (1977) Paleomagnetic field intensity variation recorded in a Brunhes epoch deep-sea sediment core, *Nature, 266, 156-159.*

King, R.F., & Rees, A.I., (1966) Detrital magnetism in sediments: an examination of some

theoretical models, *J.Geophys. Res., 71, 561—572.*

Kristjansson, L., Fridleifsson, I.B., & Watkins, N.D. (1980), Stratigraphy and paleomagnetism of the Esja, Eyrarfjall and Akrafjall Mountains, SW-Iceland; *J. Geophys., 47, 31—42.*

Langel, R.A., (1985) Chapter Three: Main Field, *submitted to Academic Press for inclusion in multi-volume work on Geomagnetism*, J.A. Jacobs, Editor.

Langel, R.A., Estes, R.H., Mead, G.D., Fabiano, E.B., and Lancaster, E.R., (1980) Initial geomagnetic field model form Magsat Vector data, *Geophys. Res. Lett., 7, 793-796.*

Langel, R.A., Ousley, G., Berbert, J., Murphy, J., & Settle, M., (1982) The magsat mission, *Geophys. Res. Lett., 9, 243-245.*

Langel, R.A. & Estes, R.H. (1982), A Geomagnetic Field Spectrum; *Geophysical Research Letters, 9, 250—253.*

Lee, S., (1983) *A study of the time-averaged paleomagnetic field for the past 195 million years*, Ph. D. Thesis, Australian National University.

Livermore, R.A., Vine, F.J., & Smith, A.G., (1983) Plate motions and the geomagnetic field —I. Quaternary and late Tertiary, *Geophys.J. Roy. astr. Soc., 73, 153-171.*

Livermore, R.A., Vine, F.J., & Smith, A.G., (1984) Plate motions and the geomagnetic field —II. Jurassic to Tertiary, *Geophys.J. Roy. astr. Soc., 79, 939-962.*

Lowes, F.J. (1974), Spatial power spectrum of the main geomagnetic field and extrapolation to the core; *Geophys. J. Roy. Astron. Soc., 36, 717—730.*

Massey, F.J. (1951), The Kolmogorov-Smirnov test for goodness of fit; *J. Amer. Stat. Assoc., 46, 68— 78.*

Mauersberger, P., (1956) Das Mittel der Energiedichte des geomagnetishcen Hauptfeldes und der Erdoberfläche und seine säkulare Änderung, *Gerlands Beitr. Geophys., 65, 207-215.*

McElhinny, M.W., & Merrill, R.T. (1975), Geomagnetic secular variation over the past 5m.y., *Rev. Geophys. Space Phys., 13, 687—708.*

McElhinny, M.W., & Senanayake, W.E., (1982) Variations in the geomagnetic dipole 1: the past 50 000 years, *J.Geomag. Geoelectr., 34, 39-51.*

McFadden, P.L. & McElhinny, M.W. (1982), Variations in the geomagnetic dipole 2: statistical analysis of VDMs for the past 5 million years; *J. Geomag. Geoelect.*, *34, 163—189.*

McFadden, P.L. & McElhinny, M.W. (1984), A physical model for paleosecular variation; *Geophys. J. Roy. Astron. Soc.*, *78, 809—830.*

Merrill, R.T., & McElhinny, M.W., (1977) Anomalies in the time-averaged paleomagnetic field and their implications for the lower mantle, *Rev. Geophys. Space Phys.*, *15, 309-323.*

Merrill, R.T., & McElhinny, M.W. (1983), *The Earth's Magnetic Field: its History, Origin and Planetary Perspective*, Academic Press.

Moffatt, H.K., (1978) *Magnetic Field Generation in Electrically Conducting Fluids*, Cambridge University Press.

Shure, L., Parker, R.L., & Backus, G.E., (1982) Harmonic splines for geomagnetic modelling, *Phys. Earth Planet. Int.*, *28, 215-229.*

Watkins, N.D., McDougall, I., & Kristjansson, L. (1977), Upper Miocene and Pliocene geomagnetic secular variation in the Borgarfjordur area of western Iceland; *Geophys. J. Roy. Astron. Soc.*, *49, 609—632.*

Wells, J.M., (1973) Non-linear spherical harmonic analysis of paleomagnetic data, in *Methods in Computational Physics,* vol. 13, *Geophysics,* edited by B.A. Bolt, pp239-269, Academic Press, New York.

Wilson, R.L., (1971) Dipole offset — the time-averaged paleomagnetic field over the past 25 million years, *Geophys. J. Roy. astr. Soc.*, *22, 491—504.*

Wilson, R.L., (1972) Palaeomagnetic differences between normal and reversed field sources, and the problem of far-sided and right-handed pole positions, *Geophys. J. Roy. astr. Soc.*, *28, 295—304.*

Wilson, R.L., & McElhinny, M.W., (1974) Investigation of the large-scale paleomagnetic field over the past 25m.y.; eastward shift of the Icelandic spreading ridge, *Geophys. J. Roy. astr. Soc.*, *39, 571-586.*

Table 1: Parameters describing preferred secular variation model.

Standard deviation in spherical harmonic coefficients (μT)

σ_1	σ_2	σ_3	σ_4	σ_l
3.00	2.14	0.86	0.37	$\dfrac{(\frac{c}{a})^{2l}\alpha^2}{(l+1)(2l+1)}$

Mean values for the spherical harmonic coefficients (μT)

g_1^0	g_2^0	g_3^0	g_4^0	g_l^0
30.0	1.8	0.0	0.0	0.0

Standard deviation in surface field components (μT)

σ_θ	σ_ϕ	σ_r
5.39	5.39	9.68

Standard deviation in non-dipole part of field components (μT)

$\sigma_{\theta_{nd}}$	$\sigma_{\phi_{nd}}$	$\sigma_{r_{nd}}$
4.48	4.48	7.6
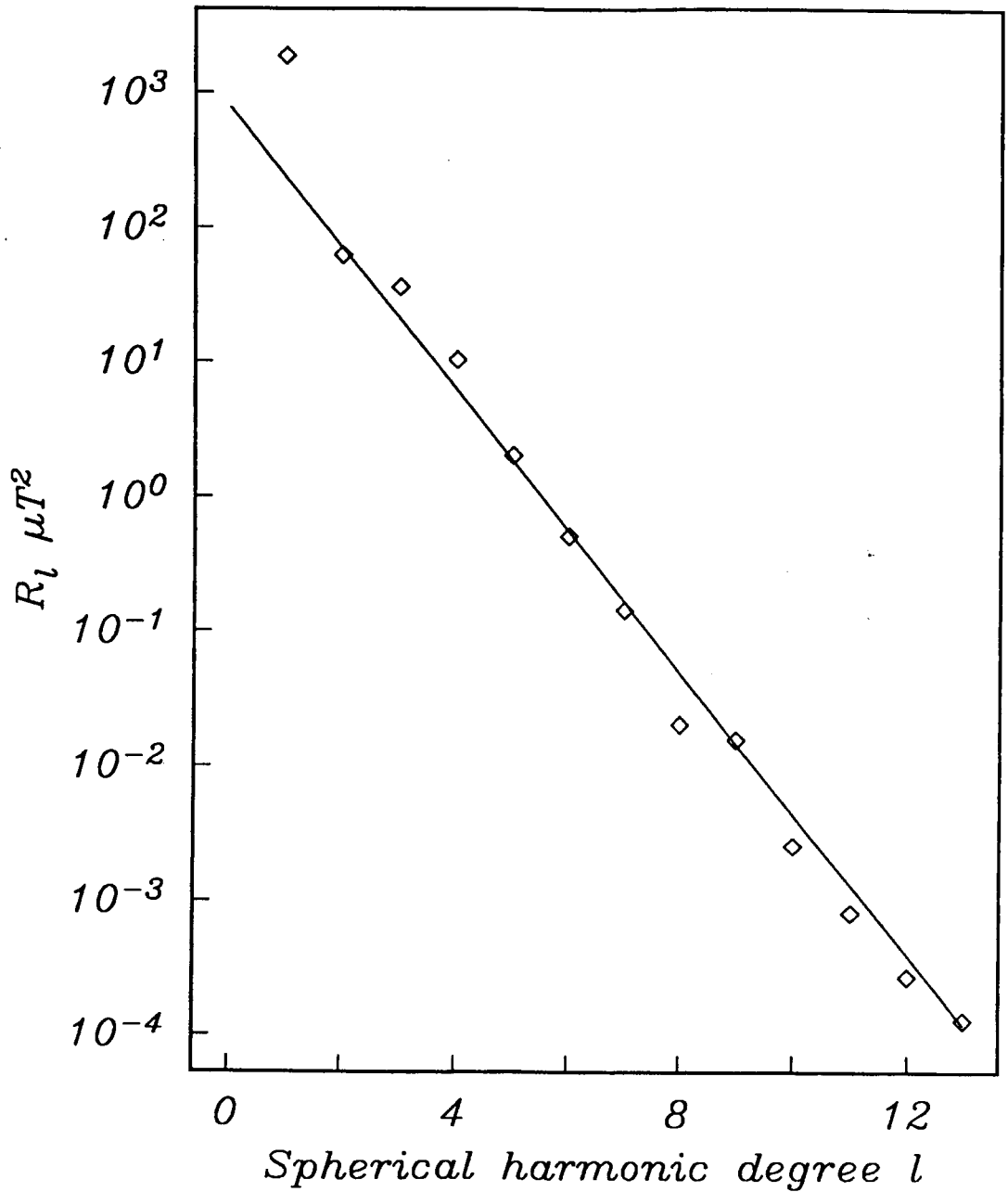
Figure 1: The geomagnetic spectrum at the Earth's surface, computed from GSFC980 magnetic field model. The fitted straight line is for a white source at the surface of the core for terms from $l=2$ to 8.
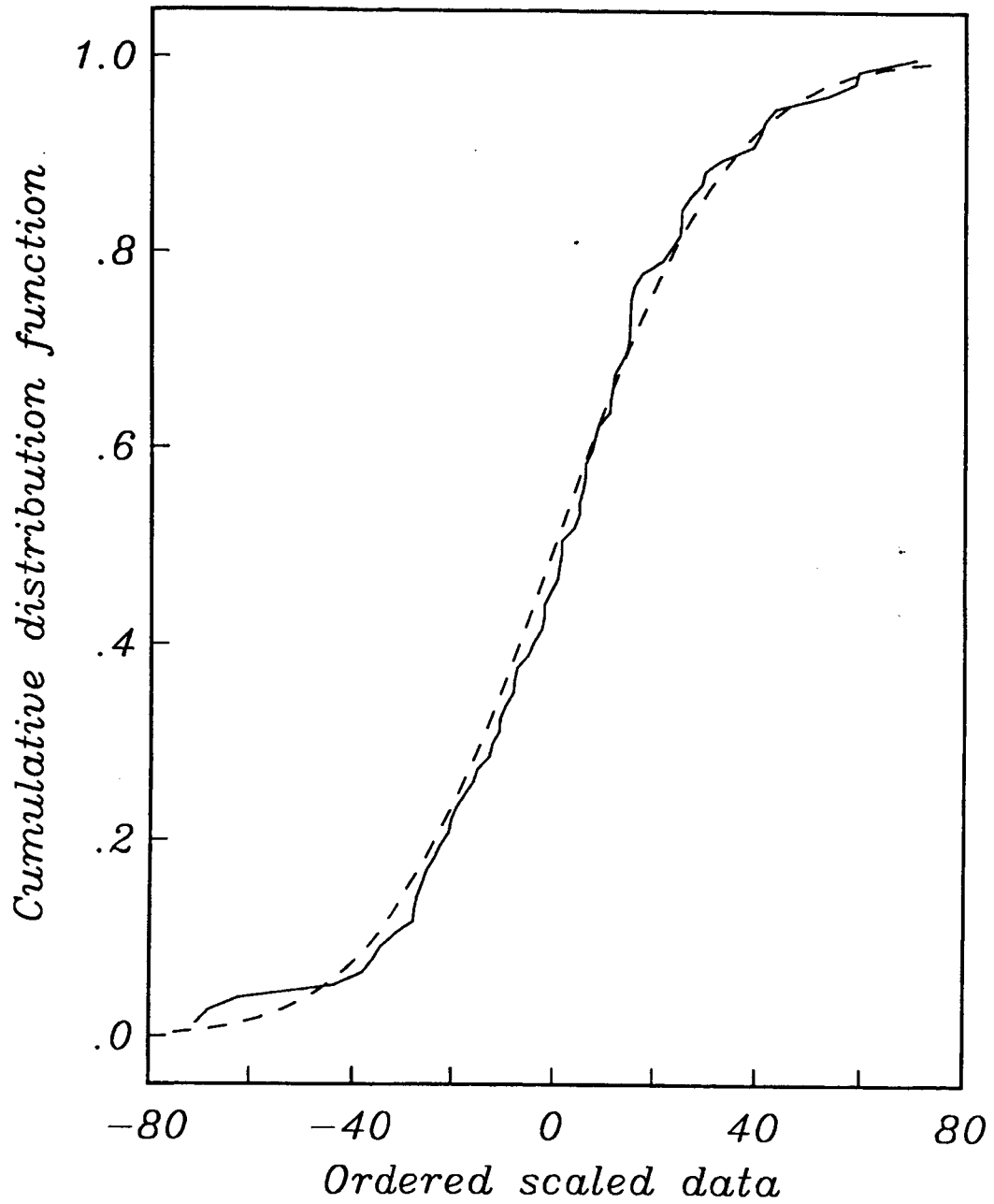
Figure 2: Empirical cdf for the GSFC980 Gauss coefficients scaled in the manner described in the text. The dashed line shows the theoretical curve expected if the scaled coefficients correspond to a Gaussian distribution.
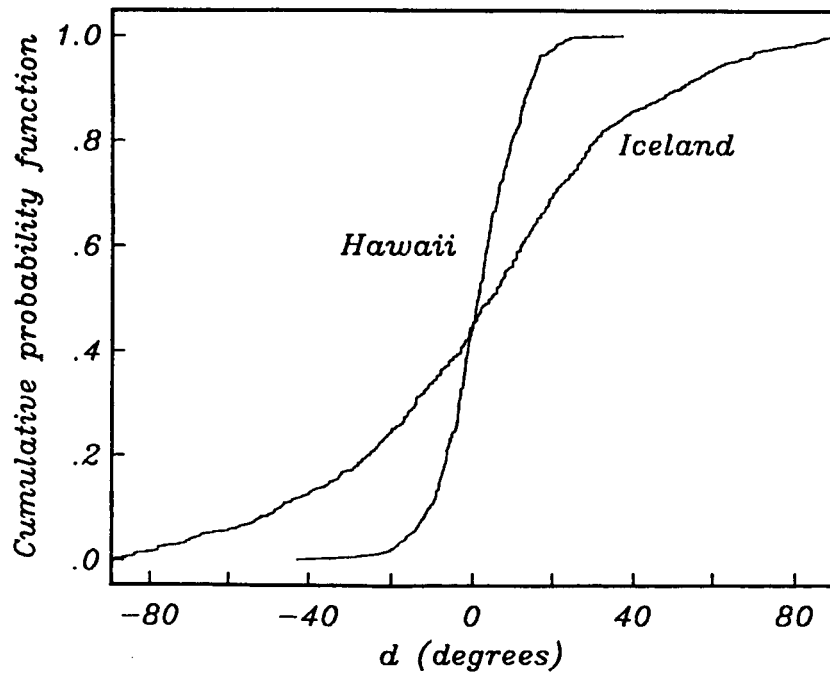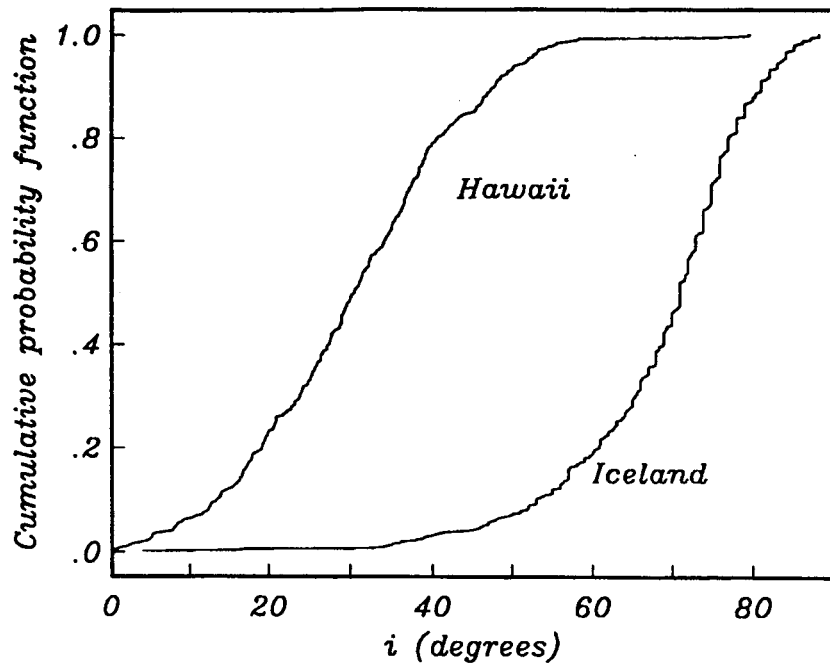
Figure 3: Empirical cumulative distribution functions for modified declination (d) and inclination (i) data from Hawaii and Iceland.
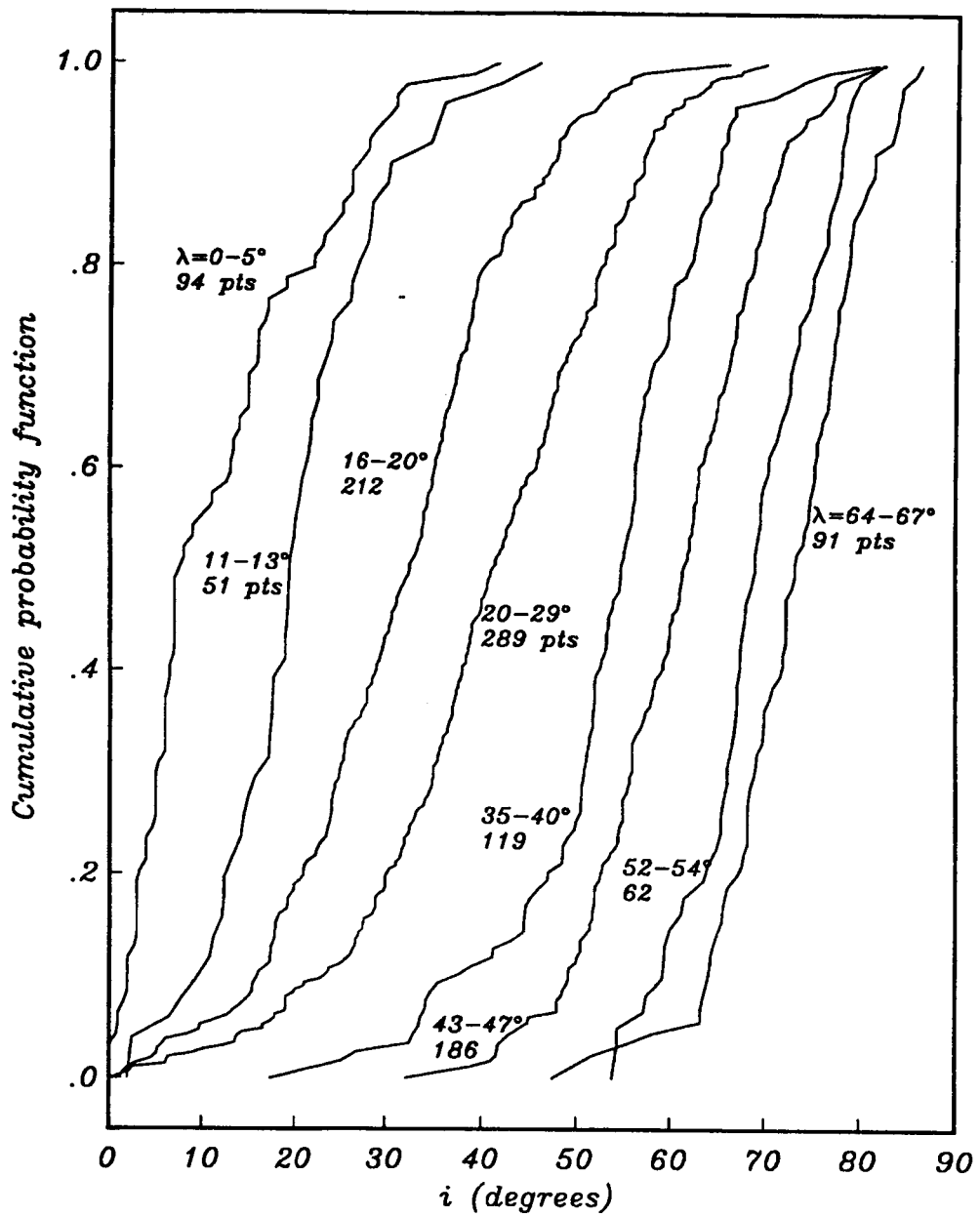
Figure 4: Empirical cdfs for modified inclination, i, using the available individual site data from Lee (1983). All the data within each indicated latitude band are combined to generate the cdf.
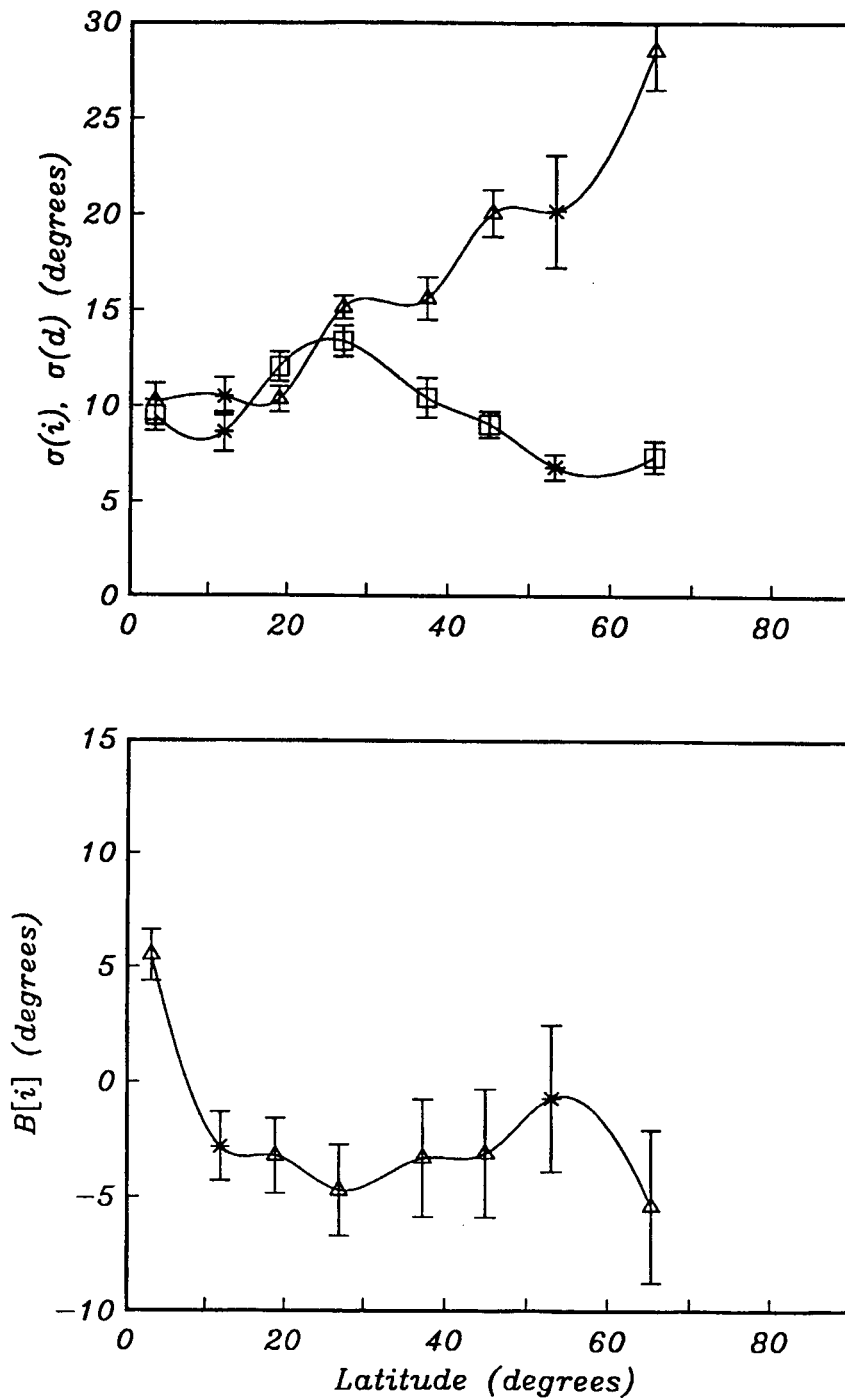
Figure 5: Bias in the modified inclination for the data grouped as in Figure 4 (lower part of figure). Data from the two smallest data groups are marked by a star to indicate their lesser reliability. Upper part shows the standard deviation in d (triangles) and i (squares) for the same data. Error bars are one standard error computed using the bootstrap technique described in the text.
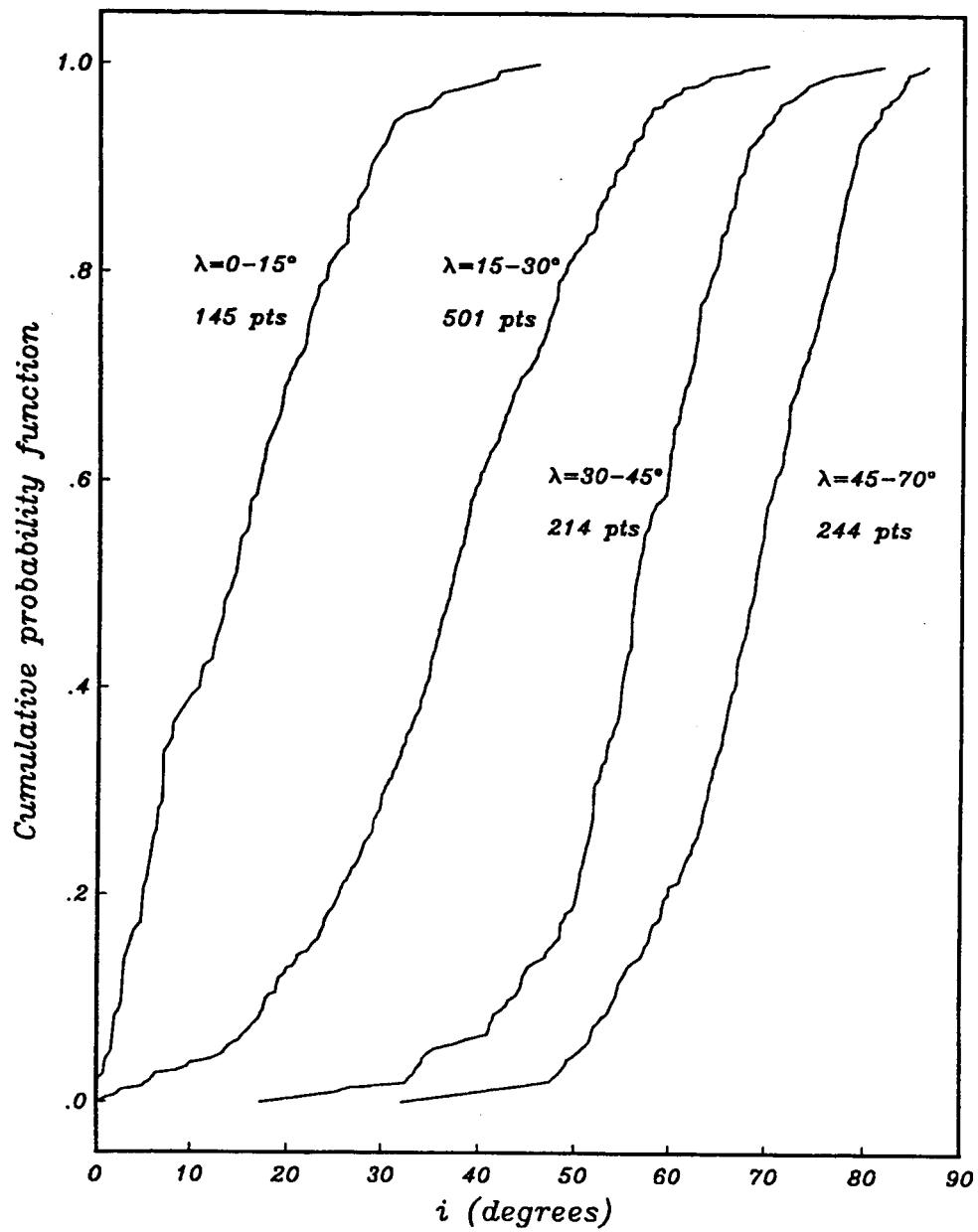
Figure 6: Empirical cdfs for i from individual site data of Lee (1983), with data grouped into wider latitude bands than in Figure 4. Note the smoother cdfs obtained.
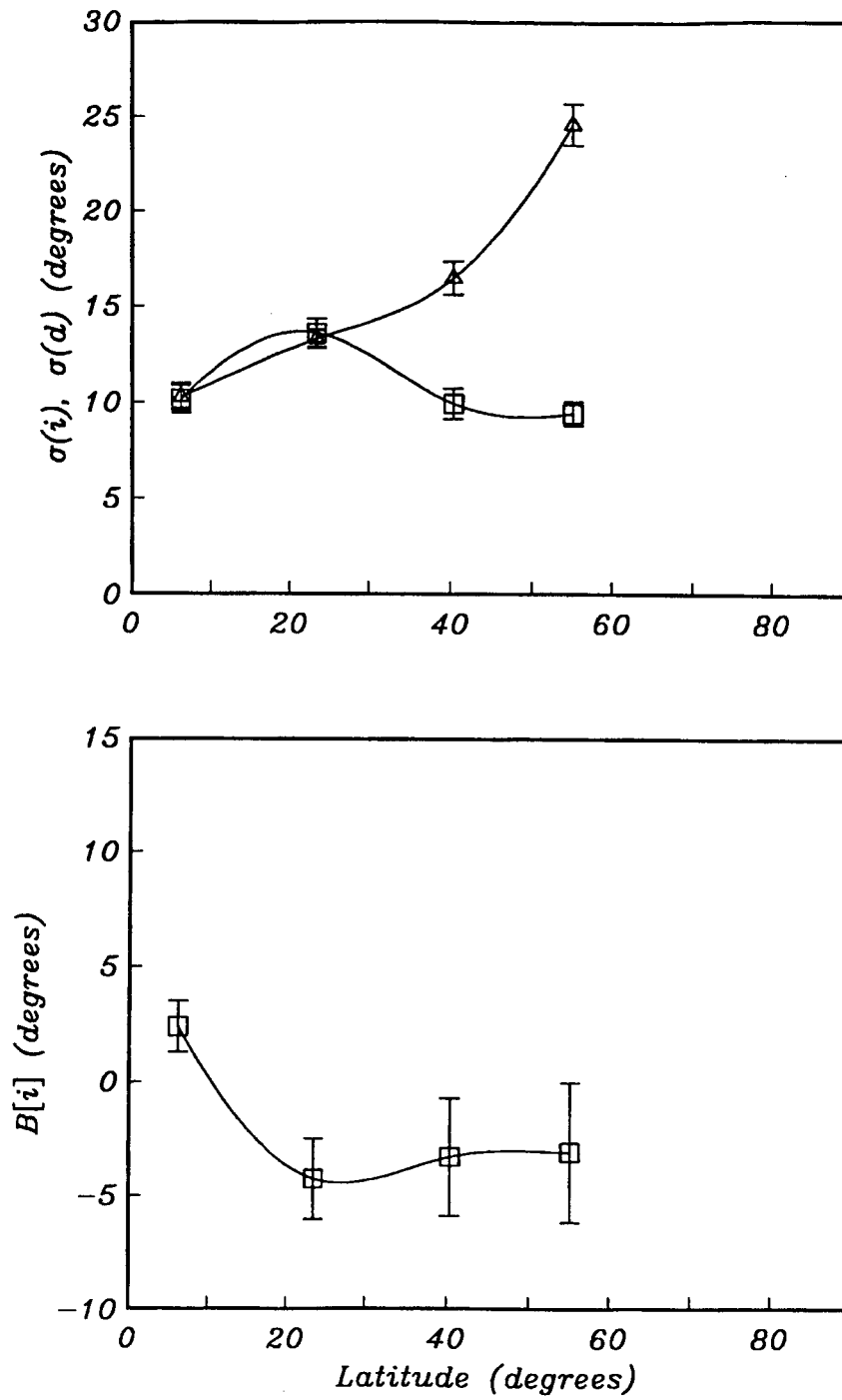
Figure 7: Bias for the modified inclination and standard deviations for d and i for the data as grouped in Figure 6.
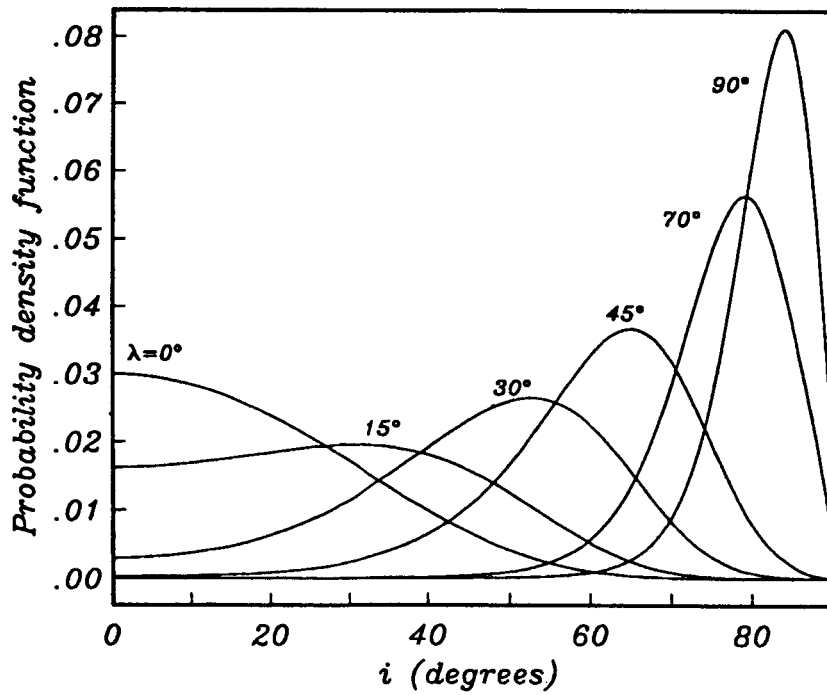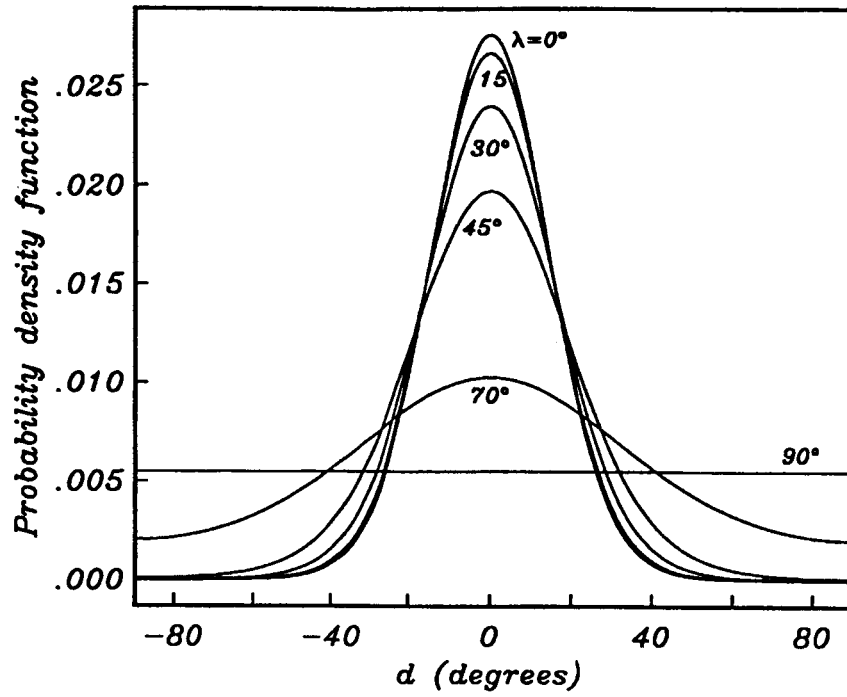
Figure 8: Probability density functions for d and i at a variety of latitudes, assuming the giant Gaussian model for the secular variation, with a mean axial dipole corresponding to the present day value.
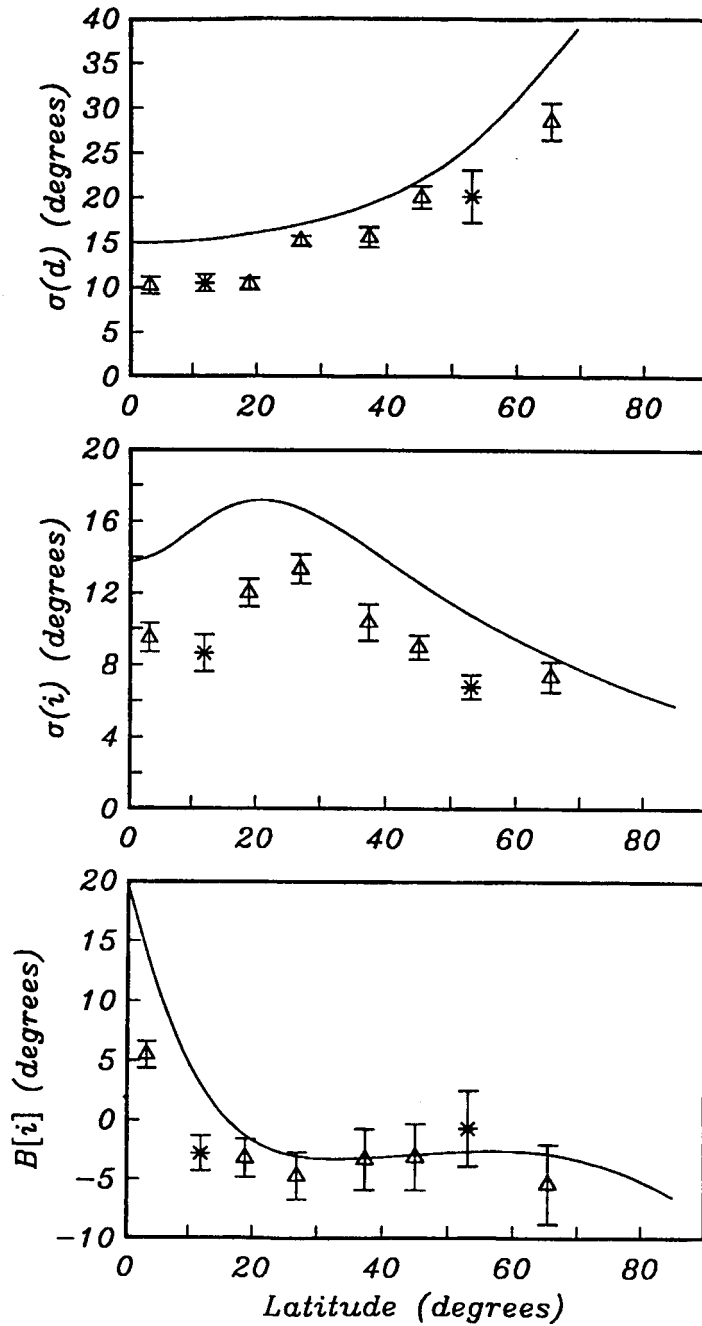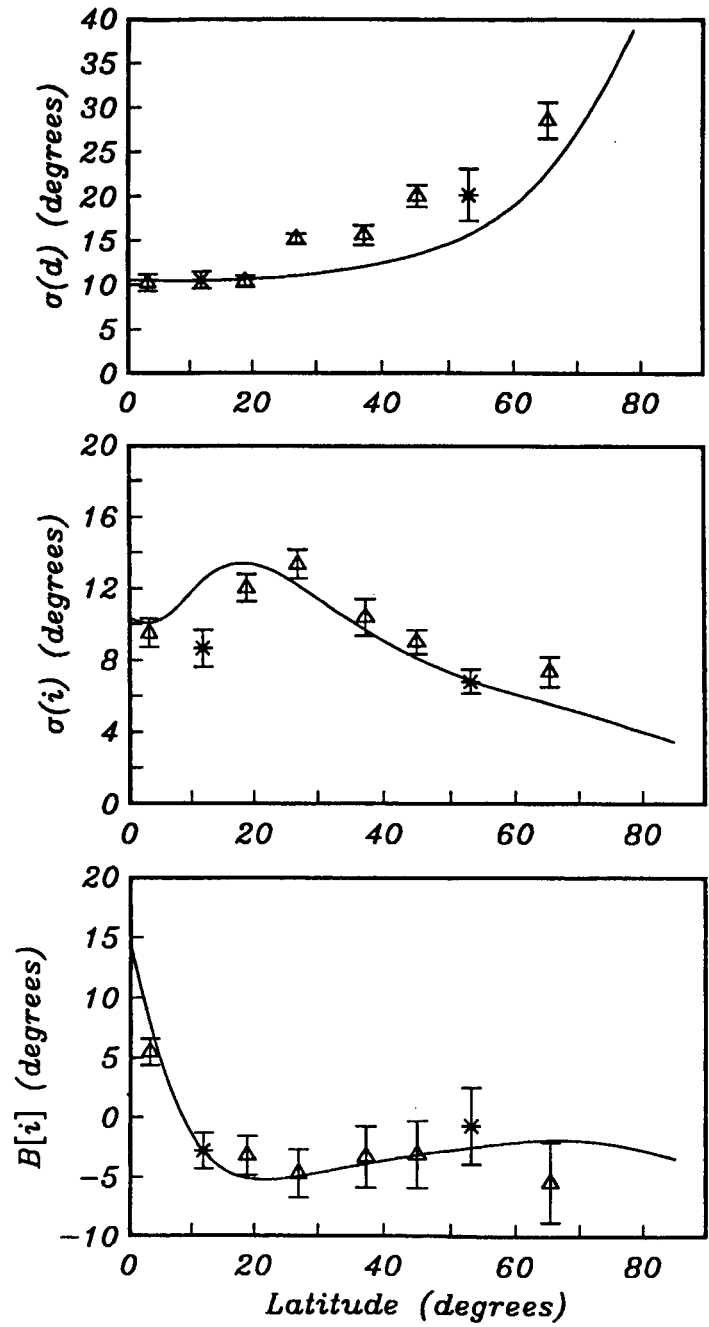
Figure 9: Bias and standard deviations as a function of latitude for
i and *d* for the model (solid line) whose pdfs are shown in **Figure 8**
and the data of Figure 4 (symbols).
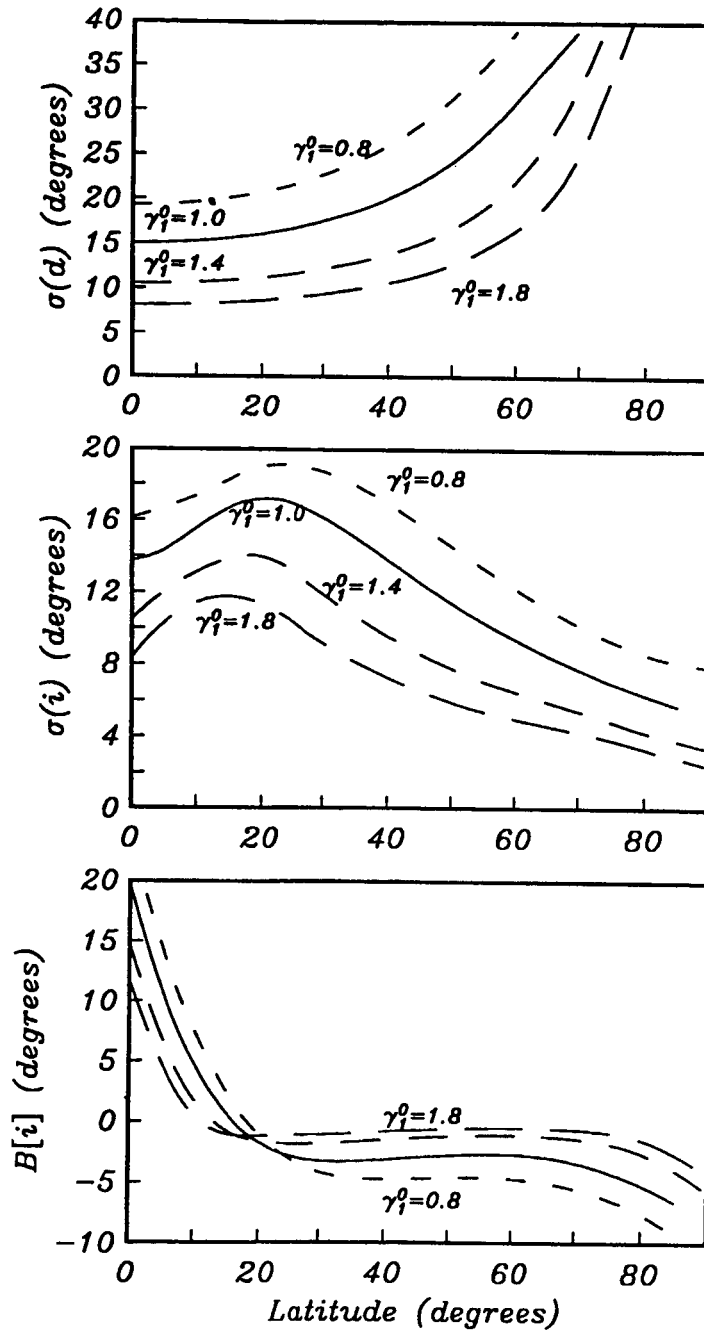
Figure 10: Effect of varying $\bar{\gamma}_1^0$ on the bias and standard deviation for the resulting i and d distributions.
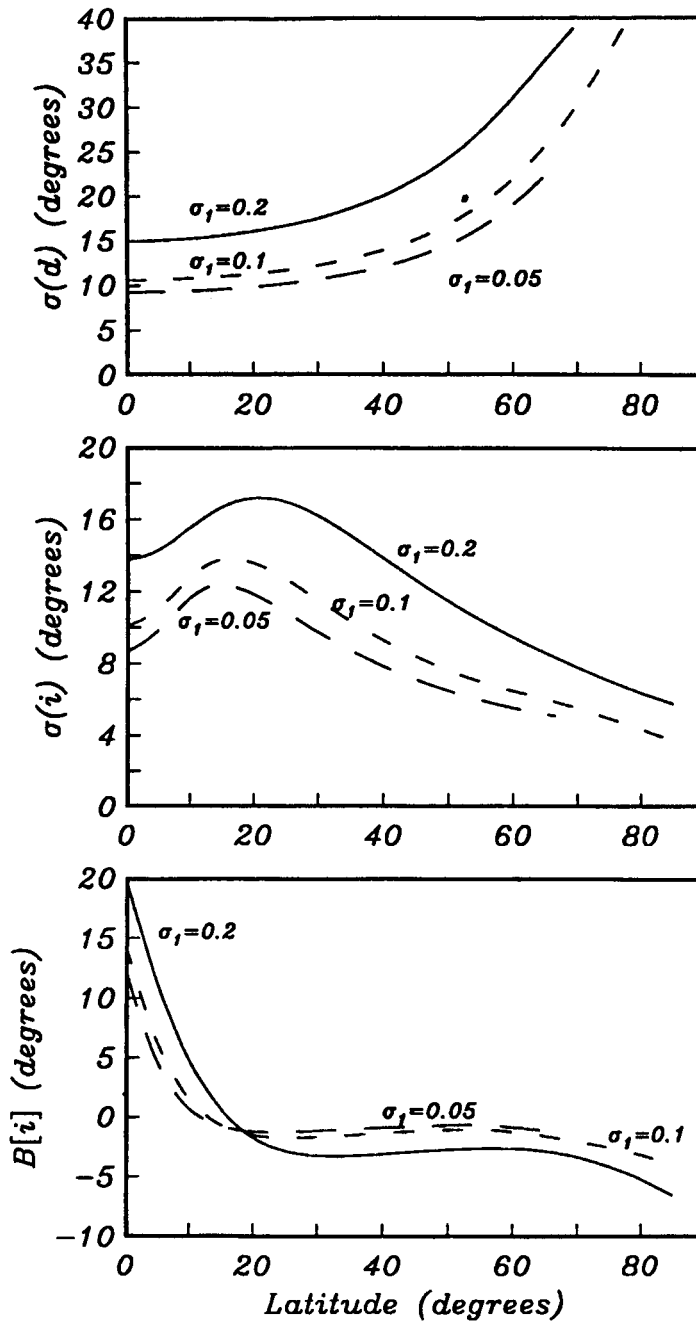
Figure 11: Effect of varying σ_1, the dipole standard deviation, on the bias and standard deviation for i and d.
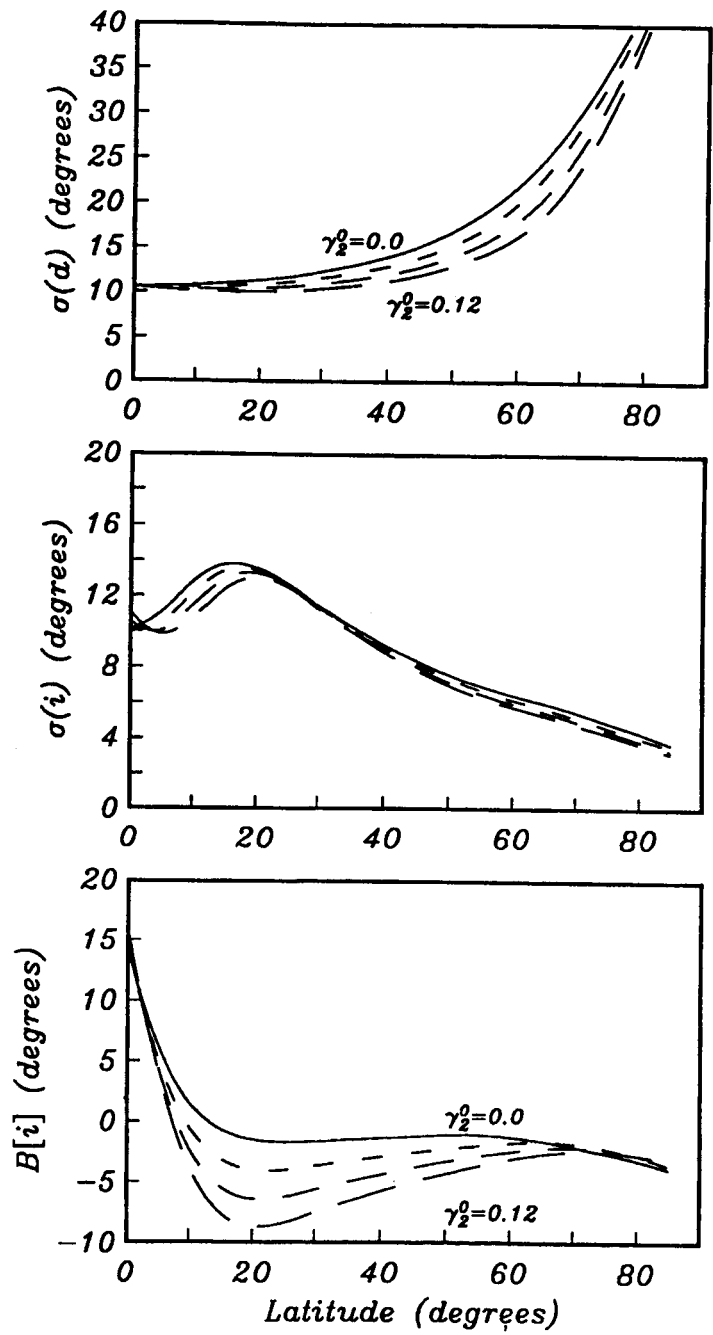
**Figure 12:** Bias and standard deviation curves resulting for various values of $\bar{\gamma}_2^0$.

Figure 13: Bias and standard deviations as a function of latitude for the preferred model described in the text. Parameters for the data compiled by Lee (1983) are again shown as open symbols.
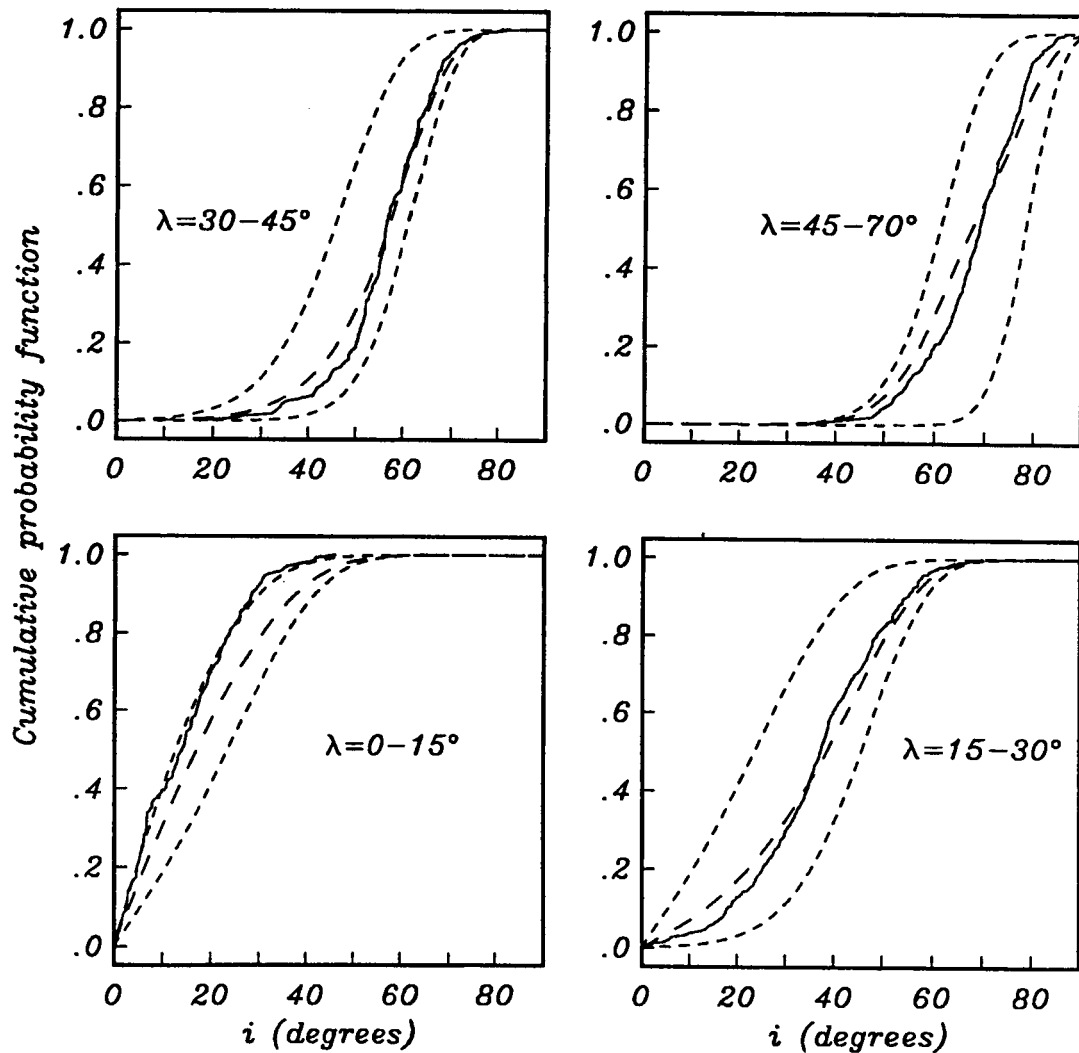
Figure 14: Cdfs for *i* data of Lee (1983) grouped as in Figure 6 (solid line) compared with the predictions of the preferred model. Long dashed lines indicate the expected average cdf from combining data at the given sites. The finely dashed lines indicate the region within which the observed cdf should lie.
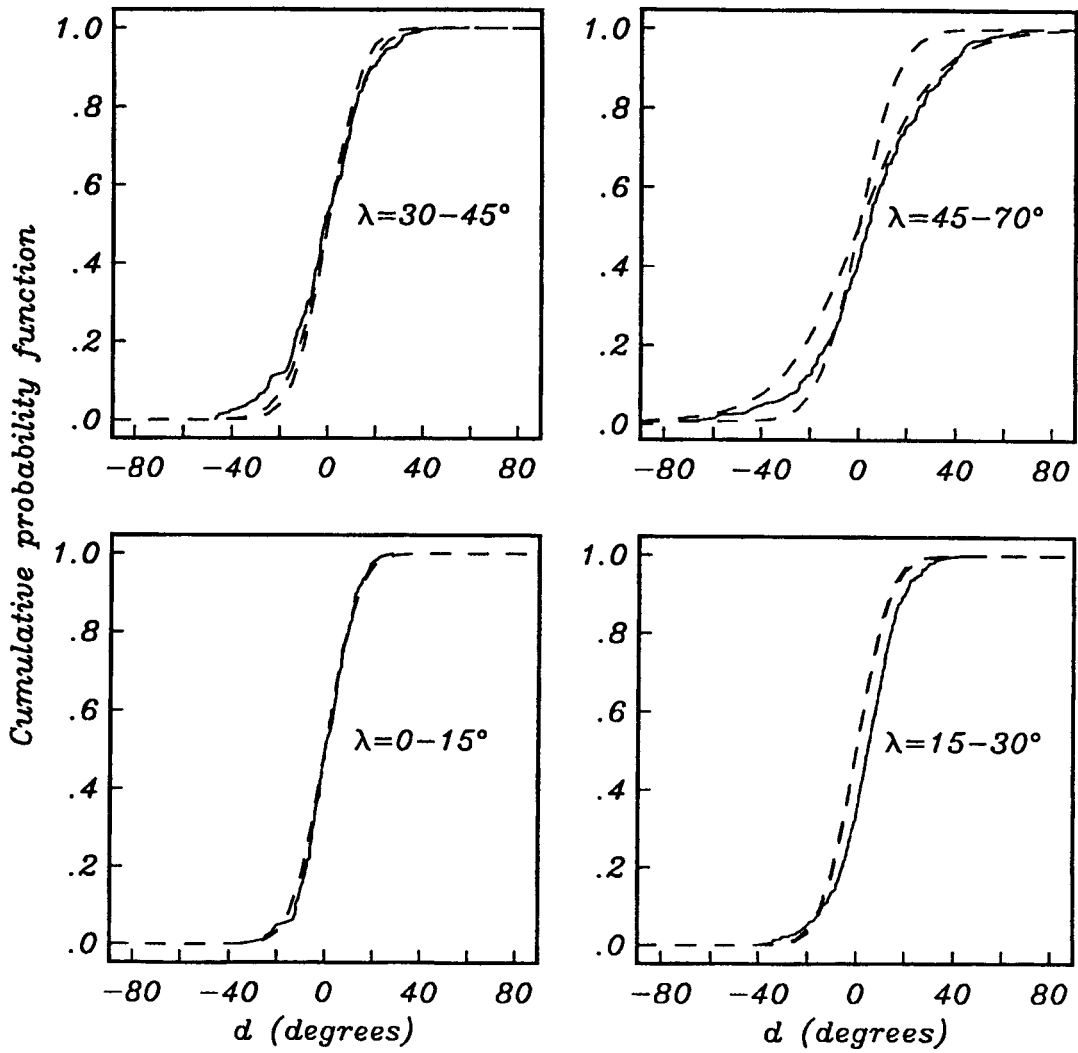
Figure 15: Cdfs for d data of Lee (1983) grouped as in Figure 6 (solid line) compared with the predictions of the preferred model. The finely dashed lines indicate the region within which the observed cdf should lie.
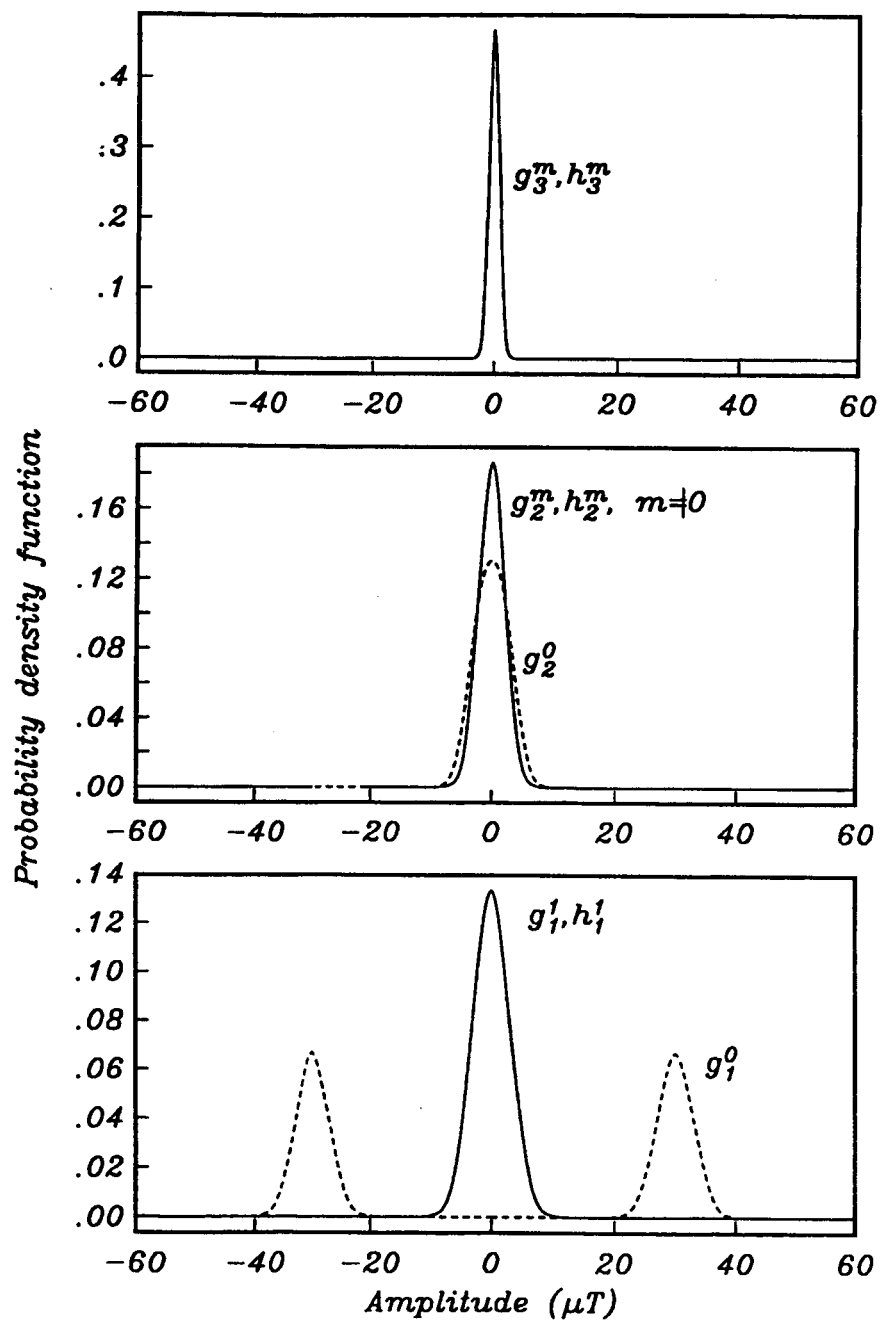
Figure 16: Statistical distribution for the first 3 degree spherical harmonic coefficients for the model. Parameters for these distributions are given in Table 1.
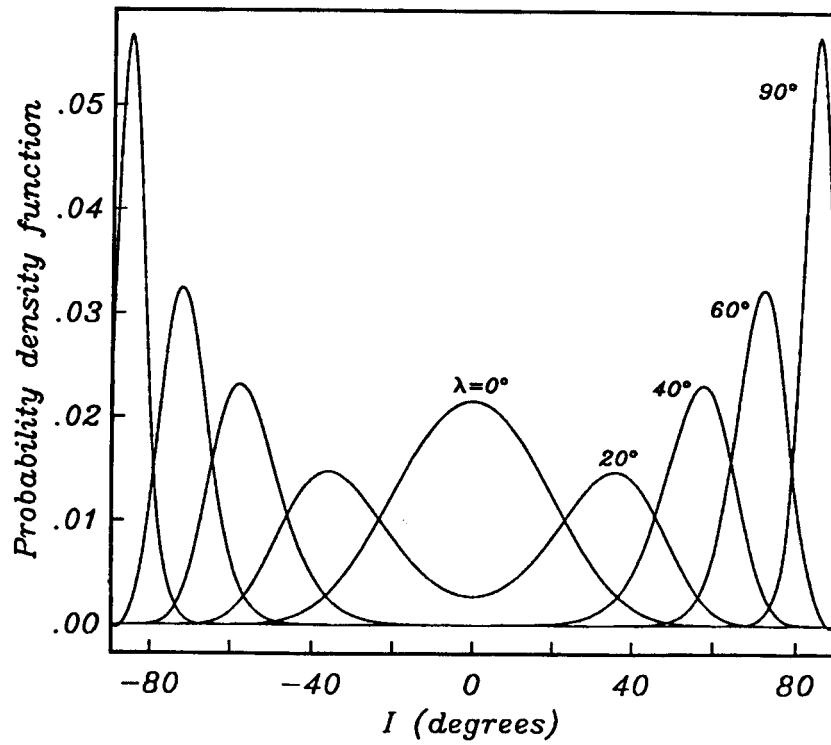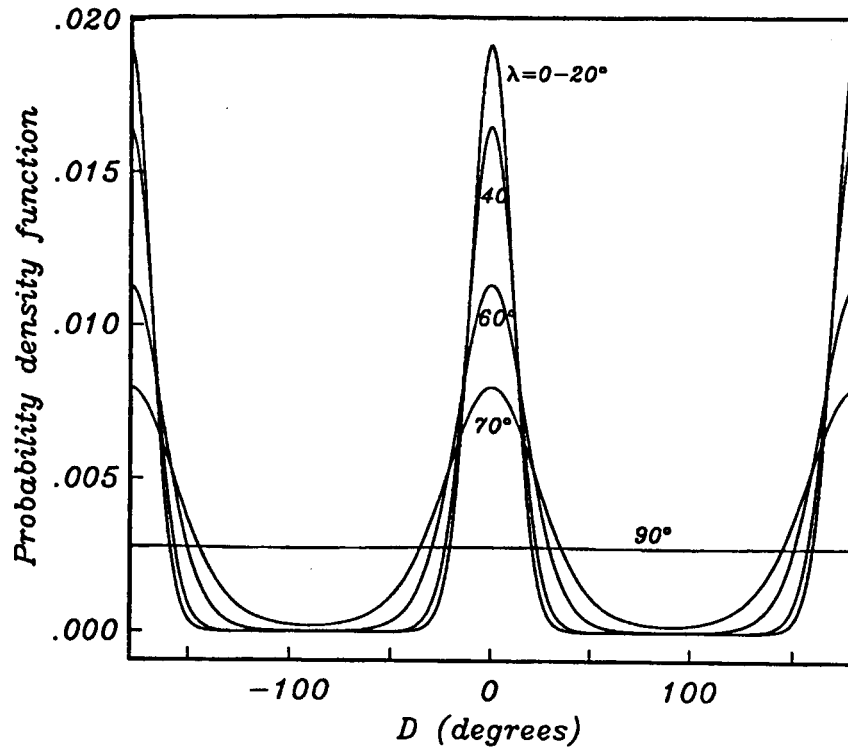
Figure 17: Probability distribution functions for declination, D, and inclination, I at a variety of latitudes for the preferred model.